Other Cardiomyopathies: Clinical Assessment and Imaging in Diagnosis and Patient Management

21

Marco Merlo, Davide Stolfo, Giancarlo Vitrella, Elena Abate, Bruno Pinamonti, Francesco Negri, Anita Spezzacatene, Marco Anzini, Enrico Fabris, Francesca Brun, Lorenzo Pagnan, Manuel Belgrano, Giorgio Faganello, and Gianfranco Sinagra

Electronic supplementary material The online version of this chapter (doi: 10.1007/978-3-319-06019-4_21) contains supplementary material, which is available to authorized users. Videos can also be accessed at http://www.springerimages.com/videos/978-3-319-06018-7.

M. Merlo (✉) • D. Stolfo • G. Vitrella • E. Abate • B. Pinamonti, MD • F. Negri
A. Spezzacatene • M. Anzini • E. Fabris • G. Sinagra, MD, FESC
Department of Cardiology, University Hospital of Trieste,
via P. Valdoni 7, Trieste 34139, Italy
e-mail: supermerloo@libero.it; davide.stolfo@gmail.com;
giancarlo.vitrella@gmail.com; abate.elena@gmail.com;
bruno.pinamonti@gmail.com; francesco_negri@yahoo.it;
anita.spe@gmail.com; marcoanzini@gmail.com;
enrico.fabris@hotmail.it; gianfranco.sinagra@aots.sanita.fvg.it

F. Brun
Department of Cardiology, University Hospital of Trieste,
via P. Valdoni 7, Trieste 34100, Italy
e-mail: frabrun77@gmail.com

L. Pagnan, MD • M. Belgrano, MD
Radiology Unit, University Hospital of Trieste,
via P. Valdoni 7, Trieste 34139, Italy
e-mail: pagny@inwind.it; belgranom@gmail.com

G. Faganello, MD
Cardiovascular Center, Azienda per i Servizi Sanitari n° 1,
via Slataper, 9, Trieste 34125, Italy
e-mail: giorgio.faganello@libero.it

B. Pinamonti, G. Sinagra (eds.), *Clinical Echocardiography and Other Imaging Techniques in Cardiomyopathies*, DOI 10.1007/978-3-319-06019-4_21,

21.1 Introduction

The nonspecific nature of the term cardiomyopathy (CMP) allows a number of diseases directly or indirectly affecting myocardial function to be included under this heading. In fact, in the classification of CMP, some myocardial diseases cannot properly be defined: dilated (DCM), hypertrophic (HCM), right arrhythmogenic (ARVC), restrictive (RCM), and infiltrative/storage CMP. These myocardial diseases are generally defined unclassified or other CMP. They are not extremely rare in clinical practice and are characterized by pathophysiologic processes that are not completely understood. Therefore, their management represents a challenge for clinical cardiologists. Interestingly, some of these CMP are characterized by partial to complete reversibility when etiologic factors are removed (reversible CMP) [1]. Finally, a peculiar form of CMP is left ventricular noncompaction (LV NC), with typical clinical–instrumental characteristics that are not yet widely known.

21.2 Peripartum Cardiomyopathy

The definition of peripartum CMP was first established according to the following four criteria adapted from the study by Demakis et al. [2]:

- Development of heart failure (HF) in the last month of pregnancy or within 5 months of delivery
- Absence of an identifiable cause for HF other than pregnancy
- Absence of recognizable heart disease before the last month of pregnancy (requiring imaging data)
- Left ventricular systolic dysfunction demonstrated by classic echocardiographic criteria, such as depressed shortening fraction or ejection fraction in the last month of pregnancy or within 5 months of delivery [3]

Peripartum CMP remains an exclusion diagnosis (all other causes of HF must be ruled out), and it seems to be linked with several risk factors, such as one or more prior pregnancies, multifetal pregnancy, older maternal age, and high blood pressure [4]. Many etiological processes occurring during pregnancy have been suggested as being causative, such as viral myocarditis, coronary artery spasm, small-vessel disease, abnormal immune response to pregnancy, and excessive prolactin excretion [4].

Common echocardiographic findings of peripartum CMP include globally decreased LV systolic function and LV enlargement, usually without LV hypertrophy (Clips 21.1a, 21.1b, 21.1c, and 21.1d). The primary echocardiographic diagnostic criteria are LV systolic dysfunction [LV ejection fraction (EF) <0.45 and/or M-mode fractional shortening <30 %) and LV dilatation (LV end-diastolic diameter >2.7 cm/m^2) between the last month of pregnancy and the first 5 months postpartum in the absence of other known causes of systolic HF [3]. Additionally, LV thrombus is not rare in patients with LV EF <35 % [5]. Peripartum CMP is frequently associated with preeclampsia (22 % vs 3–5 % in the general population) [6]. In this context marked LV hypertrophy can be exceptionally observed (Fig. 21.1, Clips 21.2a, 21.2b, 21.2c, 21.2d, 21.2e, 21.2f, 21.2g, 21.2h, and 21.2i), which is usually reversible, such as impaired LV contractility.

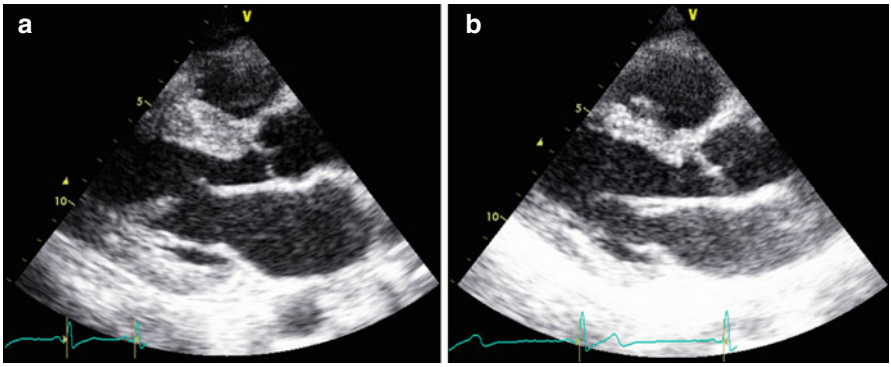

Fig. 21.1 (**a**, **b**) Echocardiographic study in a 42-year-old woman with peripartum cardiomyopathy associated with preeclampsia. Parasternal long-axis view (**a**), diastolic frame, of the first echocardiogram postdelivery documenting severe left ventricular (LV) hypertrophy (septal wall thickness 17 mm, posterior wall thickness 14 mm), with diffuse hypokinesis and severe systolic dysfunction [fractional shortening 15 %, ejection fraction (EF) 32 %]. After 6 months of therapy with beta-blocker and angiotensin-converting-enzyme inhibitor, echocardiography in the parasternal long-axis view, diastolic frame (**b**) shows normal LV wall thickness (septal wall thickness 9 mm, posterior wall thickness 9 mm), with normal regional wall motion and systolic function (fractional shortening 39 %, EF 64 %)

There are few data about the use of advanced echocardiographic technologies in this disease. A similar counterclockwise rotation during systole of both the base and the apex at speckle-tracking analysis was reported in one case of peripartum CMP associated with LV NC [7]. This subtle deformation abnormality has been interpreted as secondary to dysfunction of basal and midwall subepicardial fibers, with resultant predominant effect exerted by the subendocardial fibers in this region. These abnormalities were reversible after optimal medical therapy. However, further investigation is required.

Studies on cardiac magnetic resonance (CMR) in the acute phases of peripartum CMP show the presence of edema at T2 sequences and on early gadolinium enhancement, suggesting an inflammatory etiology for this condition. In addition, late gadolinium enhancement (LGE) seems to identify cases with unfavorable prognosis [8, 9].

Although peripartum CMP shares many features with other forms of nonischemic CMP, women affected by this disease have a higher rate of spontaneous recovery of LV function [5]. Monitoring patients after diagnosis should include serial echocardiograms to identify improvement in systolic function in response to conventional HF medical treatment. Less severely impaired LV EF and lower LV dimensions at the time of diagnosis are predictors of complete LV function recovery and good outcome [10].

Previous studies assessed prognostic implications of LV contractile reserve at initial diagnosis and demonstrated that improved LV EF during dobutamine stress echocardiography accurately correlates with subsequent recovery of LV function and confers a benign prognosis to this CMP [11].

The existing literature indicates that many patients with peripartum CMP actually have myocarditis. The diagnosis of myocarditis is more suspicious in the presence of progressive worsening of LV dilation and systolic dysfunction at serial echocardiographic evaluations. In these cases, endomyocardial biopsy (EMB) can be useful to modify therapeutic strategies.

Finally, one important question asked by women with a history of this disease is whether they can safely get pregnant again. For women with persistently reduced LV EF, there is a substantial risk of recurrent HF. On the other hand, for women who recover, the risk is much lower and can be further stratified by a stress echocardiogram: in the presence of normal contractile reserve, the risk of recurrent disease or HF seems to be low [4].

21.3 Tako-Tsubo Cardiomyopathy

Tako-tsubo, or stress-induced CMP, is an acute, usually reversible, disorder of the heart characterized by transient LV dysfunction [12–15]. Clinical presentation is usually similar to an acute coronary syndrome, with precordial pain and dyspnea. Other symptoms may include palpitations, syncope, or even cardiac arrest or sudden death (SD). A trigger, such as a stressful physical or psychological event, can usually be detected in 27–100 % of cases. Many diagnostic criteria have been formulated, but the most widely accepted are those of the Mayo Clinic in the United States [13], which require normality of the epicardial coronary arteries. Tako-tsubo syndrome may be confused with stress syndrome caused by underlying pheochromocytoma, and attention should be paid to this clinically important differential diagnosis. The etiology and pathogenesis are presently unknown. One possibility is stress-induced catecholamine release, producing cardiac stunning through direct toxic damage to myocytes and/or vasoconstriction with ischemia [16]. The apical region is the most vulnerable area, probably due to the large number of adrenergic receptors [14]. Treatment is symptomatic and is determined by the complications occurring during the acute phase. Complications are estimated to occur in 19 % of cases, mortality varies between 0 and 12 % [15], and recurrence is rare.

Echocardiography plays a major role in achieving this diagnosis. In fact, the most salient feature of this disease is the unusual LV contractile pattern noted at the time of admission. Typically, it is characterized by a transient hypokinesis, akinesis, or dyskinesis of the LV apical and mid segments, usually with compensatory hyperkinesia of the basal portions (Fig. 21.2, Clip 21.3a) [17]. Moreover, regional wall motion abnormalities (WMA) extend beyond a single epicardial vascular distribution [18]. Global contractile LV function is usually significantly impaired. The time course for cardiac function improvement is variable, from a few days to several weeks; however, LV function typically recovers completely (Fig. 21.2, Clip 21.3b).

Atypical forms of stress-induced CMP have been increasingly reported. Transient midventricular ballooning with preserved basal and apical contractility (inverted tako-tsubo CMP) has been described [19]. Additionally, LV apical thrombosis may occur during the early stage of the disease due to transient apical akinesis and

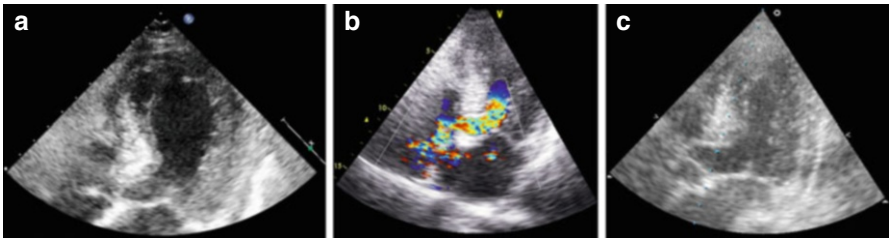

Fig. 21.2 (**a**–**c**) A 79-year-old woman with tako-tsubo-like cardiomyopathy. Echocardiography at the time of admission shows left ventricular (LV) apical akinesis, hypokinesis of the mid segments with compensatory hyperkinesis of the basal portions, and moderate systolic dysfunction (**a**) in the apical four chamber view, systolic frame. Apical long-axis view (**b**) recorded with color-Doppler imaging demonstrates marked turbulence in the LV outflow tract (OT), consistent with dynamic LV OT obstruction in the presence of a sigmoid interventricular septum. An echocardiogram performed 4 months later shows complete recovery of LV wall motion and systolic function (**c**) in the apical long-axis view, systolic frame

aneurysm formation [20]. The use of contrast agents can be particularly helpful to highlight apical thrombosis and if there is a difficult acoustic window.

Dynamic LV outflow tract (OT) obstruction is a relatively common complication of stress-induced CMP, with a reported incidence of >10 % (Fig. 21.2, Clip 21.3c) [21]. There are probably some predisposing factors to LV OT obstruction, i.e., sigmoid interventricular septum or a small LV or LV OT; more importantly, this complication is frequently precipitated by certain conditions, such as hypovolemia, ionotropic drugs, and counterpulsation.

Stress-induced CMP is also frequently complicated by acute mitral regurgitation (MR). Systolic anterior motion (SAM) of the mitral valve (MV) is typically associated with LV OT gradient and accounts for one half of acute MR. MV tethering with increased valve tenting area the in presence of LV systolic dysfunction and LV enlargement has been proposed as an alternative mechanism responsible for MR in this disease [22].

Right ventricular (RV) involvement and dysfunction is relatively common and is associated with lower LV EF [23]. Conversely, ventricular rupture is an extremely rare life-threatening complication of stress-induced CMP. There are a few cases reported in literature, principally in elderly female patients [24].

Myocardial viability and contractile reserve could be evaluated with low-dose dobutamine stress echocardiography in suspected stress-induced CMP. However, particular caution must be taken considering that increasing doses of dobutamine can worsen LV OT gradient. Furthermore, the possible occurrence of tako-tsubo CMP as a complication of dobutamine stress echocardiography has been reported [25].

Finally, if transthoracic echocardiography (TTE) is limited by poor acoustic windows, transesophageal echocardiography (TEE) can provide clearer image quality and allows careful evaluation of MV anatomy and full definition of the MR [17].

Advanced echocardiographic techniques could be useful in diagnosis and prognostic stratification of tako-tsubo CMP. Both 2D and 3D imaging allows recognition of the contractile pattern, mainly when the apex is involved; 3D imaging

may allow better visualization of contracting and noncontracting segments when medial segments are involved. Myocardial contrast echocardiography seems to be a useful tool by which to clarify the mechanisms involved the myocardial injury and to distinguish stress-induced CMP from acute coronary syndrome. In one study, myocardial perfusion was relatively preserved in patients with tako-tsubo CMP compared with those with myocardial infarction. The authors of that study concluded that myocardial contrast echocardiography had a high sensitivity, specificity, and positive and negative predictive values for detecting stress-induced CMP (91, 86.2, 83, and 93 %, respectively) [26]. In addition, transient impairment of coronary flow reserve, assessed by Doppler coronary flow analysis during dipyridamole test, has also been reported in this disease [27]. Finally, at 2D strain by speckle-tracking analysis, a progressive decrease of longitudinal strain values from base to apex was reported in patients with classical stress-induced CMP [17].

CMR in this CMP exhibits the characteristic finding of transmural high T2 signal in the midanterior wall and apical segments, matching the distribution of WMA [28, 29]. This abnormality can persist after 3 months from the acute event although is substantially decreased compared with the acute phase [30]. Myocardial inflammation may also be found at global relative enhancement and quantitative T1 mapping sequences [31, 32].

Patients with tako-tsubo CMP usually do not exhibit hypoenhancement at first-pass perfusion [33], or by LGE [34, 35], thus helping differentiate this condition from acute myocardial infarction with spontaneous coronary recanalization or acute myocarditis [35]. When LGE is found, it is focal or patchy and has decreased signal intensity compared with ischemic LGE [36, 37]. This finding is usually indicative of a more severe acute condition, which tends to resolve within 6 months [38].

CMR data from a large multicenter registry of patients with tako-tsubo CMP revealed four distinct patterns of regional ventricular ballooning [36]:

- Apical (82 %)
- Biventricular (34 %)
- Midventricular (17 %)
- Basal (1 %)

Single-photon-emission CT (SPECT) findings include reduced apical perfusion assessed with technetium-99 m (^{99m}Tc)-tetrofosmin in the acute phase, which recedes during follow-up [39–41]. Severely impaired myocardial fatty-acid metabolism assessed with ^{123}I-beta-methyl-p-iodophenyl pentadecanoic acid (^{123}I-BMIPP) [42–44], and apical sympathetic dysinnervation in the acute phase assessed by ^{123}I-metaiodobenzylguanidine (MIBG) uptake [43, 45–47] were also found, mismatched from perfusion defects.

Positron emission tomography (PET) studies also report perfusion/metabolism mismatch involving the apical akinetic area assessed by [^{18}F]-fluorodeoxyglucose (FDG) and [^{13}N]-ammonia or by thallium-201 radiochemical thallium chloride (^{201}Tl) SPECT [48–50]. Glucose metabolism assessed by [^{18}F]-FDG PET and sympathetic function assessed by [^{123}I]-MIBG SPECT seem to be strictly correlated in affected segments [46].

In tako-tsubo CMP, LV apical WMA is typically transient and resolves over a period of days to weeks. Therefore, follow-up echocardiographic reevaluation is essential to monitor its resolution and recovery of LV systolic function. The prognosis is generally favorable; reported in-hospital mortality rates range from 0 to 8 % [18]. As it is difficult to predict subsequent occurrence of complications immediately after the onset of the disease, serial echocardiographic evaluations should be performed during the in-hospital period. There is no established consensus on how to manage stress- induced CMP, but early detection of complications, such as the occurrence of LV OT gradient or apical thrombosis, can protect against a poor outcome and may lead to some changes in therapeutic strategies.

In this disease, RV involvement is relatively common, and RV dysfunction is associated with lower LV EF, longer hospitalization, more complications, such as severe HF, and need for intra-aortic balloon pump and cardiopulmonary resuscitation [23]. LV EF at admission is one of the independent predictors of mortality [51]. Moreover, absence of LV function recovery within 1 week was an independent factor associated with mortality [52]. Other prognostic indicators of worse outcome are intraventricular thrombus formation and LV OT gradient occurrence [17]. Recurrence of stress-induced CMP occurs in approximately 10 % of patients [53] and is unpredictable from imaging data at first manifestation.

21.4 Tachycardia-Induced Cardiomyopathy

Tachycardia-induced CMP (TIC) is a frequent cause of reversible HF secondary to persistent supraventricular or ventricular arrhythmias and in the absence of preexisting structural heart disease [54]. Early diagnosis is crucial for prompt reestablishment of sinus rhythm and normal heart rate, with consequent improvement or even normalization of myocardial function. The pathogenesis is still controversial: Elevated heart rate causes structural alterations of myocytes, mitochondrial abnormalities, oxidative stress, and loss of contractile tissue due to necrosis or apoptosis. Moreover, tachycardia reduces myocardial perfusion, leading to myocardial stunning, interstitial fibrosis, and neurohumoral variations with elevations in natriuretic peptide, endothelin, catecholamines, and the renin-angiotensin-aldosterone system (RAAS).

Strict clinical and echocardiographic follow-up is very important in order to recognize relapses, which tend to be more severe and life threatening. Furthermore, due to the fact that LV remodeling can occur despite EF and heart rate normalization, long-term treatment with beta-blockers and angiotensin-converting enzyme (ACE) inhibitors is recommended.

In TIC, imaging techniques are essential to exclude other causes of ventricular dysfunction and to assess its reversibility after normalization of atrial or ventricular rate; echocardiography, being widely available and inexpensive, is the cornerstone in establishing the presence of LV dysfunction and narrowing the list of differential diagnoses. LV systolic dysfunction is the typical model of presentation. However, other aspects can sustain the diagnostic hypothesis. Usually, myocardial thickness

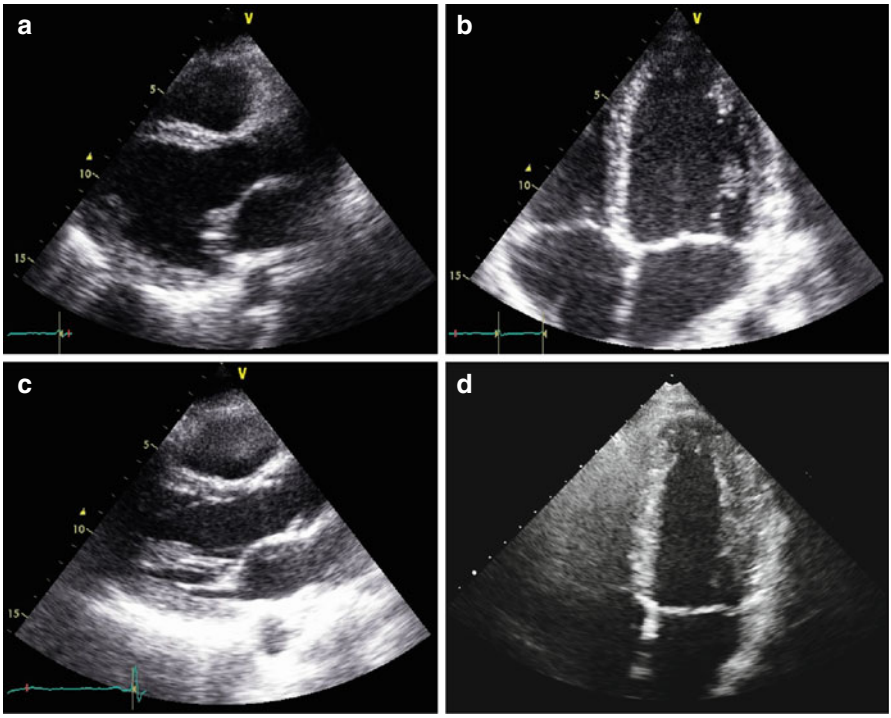

Fig. 21.3 (**a**–**d**) Echocardiographic study in a 32-year-old patient with atrial fibrillation (AF) and tachycardia-induced cardiomyopathy. Echocardiogram shows mild left ventricular (LV) dilation [end-diastolic diameter corrected for body surface area (BSA) 32 mm/mq), with normal wall thickness, diffuse hypo-akinesis, and severe systolic dysfunction [ejection fraction (EF) 22 %] in the parasternal long-axis (**a**) and apical four-chamber views (**b**), systolic frames. The echocardiogram performed 5 months after successful radiofrequency catheter ablation of AF shows normal LV dimensions (end-diastolic diameter corrected for BSA 26 mm/mq), wall motion, and systolic function (EF 60 %) in the parasternal long-axis (**c**) and apical four-chamber (**d**) views, systolic frames

is preserved, indicating the absence of scar tissue. Moreover, some studies suggest that the absence of severe LV dilation may support the diagnosis of TIC rather than DCM accompanied by supraventricular tachycardia (Fig. 21.3, Clips 21.4a, 21.4b, 21.4c, and 21.4d) [55, 56]. In fact, Jeong et al. [55] reported that LV end-diastolic dimension ≤61 mm could predict TIC with a sensitivity of 100 % and a specificity of 71 % in patients with HF and tachyarrhythmia.

LV diastolic dysfunction should be considered a component of TIC and is indeed sometimes the first expression of the disease [57]. However, it is particularly difficult to assess at Doppler in the presence of tachyarrhythmias. Contractile reserve at low-dose dobutamine stress echocardiography has been reported as a predictor of LV function recovery after catheter ablation of AF in TIC [58].

TEE can provide better image quality in patients with a poor acoustic window. Moreover, it is essential to identify left atrial appendage clots when restoring sinus rhythm is the chosen treatment. Finally, TEE and intracardiac echocardiography

may be helpful during catheter ablation of arrhythmias, even without fluoroscopy [59]. There are a few data regarding the application of new and advanced echocardiographic technologies in the setting of TIC. Alterations in LV torsion have been reported in an experimental model [60]. Strain and strain-rate imaging can provide detailed regional and global LA functional assessment [61]. In patients who have undergone catheter ablation for atrial fibrillation, LA strain and strain rate during atrial filling (parameters of LA reservoir function) are known to be better predictors of sinus rhythm maintenance [62]. Real-time 3D TEE has been demonstrated to be feasible during ablation procedures, allowing fluoroscopy-free navigation and precise anatomical delineation of atrial structure [63]. CMR with LGE may differentiate TIC, which seldom shows LGE from primary CMP, in which LGE is frequent [64]. Myocardial glucose metabolism assessed by [^{18}F]-FDG PET was found to be impaired in TIC [65].

The improvement of LV function after normalization of the heart rate is a hallmark of TIC. Therefore, multiple evaluations are necessary to identify changes in LV EF. Echocardiography is probably the most feasible and less expensive technique allowing close follow-up of these patients. The time course of improvement in biventricular systolic function has not been fully established; generally it can be observed soon after heart rate normalization [66]. If LV systolic dysfunction does not improve, other causes of impaired LV function must be reconsidered, justifying an "impure" form of TIC (possible association with dilated CMP, myocarditis, or ischemic heart disease).

It should be noted that patients with a history of successfully treated TIC are susceptible to a more severe CMP if the offending tachyarrhythmia recurs [67]. For this reason, patients should be periodically evaluated after complete LV function restoration.

21.5 Myocarditis

Myocarditis is an inflammatory disease of the myocardium and is diagnosed by established histological [68] (Fig. 21.4), immunological, and immunohistochemical criteria [69]. Most cases of myocarditis observed in clinical practice in the Western world are ascribable to viral infections and to the related reaction of the immune system. On the other hand, myocarditis can also be triggered by many specific causes, such as bacterial or parasitic infections, autoimmune diseases, hypersensitivity processes, hypercatecholaminergic states, drugs, toxic substances, and physical agents [69]. Clinical presentation of myocarditis is polymorphic, ranging from subclinical or benign forms to major clinical syndromes, such as severe HF or life-threatening ventricular arrhythmias. However, for simplification purposes, it can be categorized into three main patterns according to disease onset: HF, arrhythmias (hypokinetic or hyperkinetic, supraventricular or ventricular), and chest pain [70]. Moreover, myocarditis is characterized by great variability in its natural history evolution, ranging from resolution, to relapse, to development of DCM, or to unexpected SD. Patients presenting with chest pain and preserved LV function are

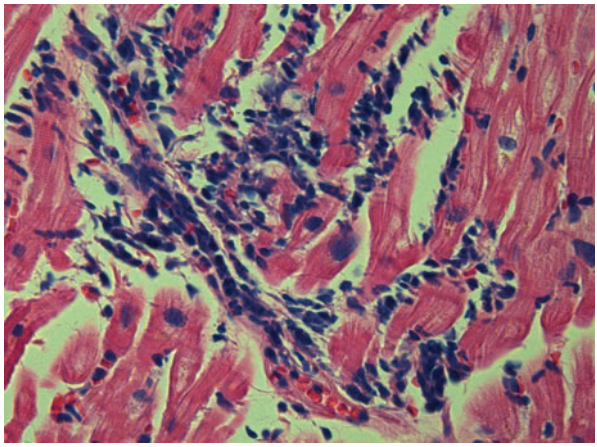

Fig. 21.4 Endomyocardial biopsy, histologic pattern, in a case of myocarditis (hematoxylin and eosin ×40). Severe lymphocytic infiltrates are present and are associated with "fraying" of myocytes (Dallas criteria)

projected through a favorable natural history, whereas those presenting with HF and significant LV dysfunction are generally characterized by a worse prognosis. On the other hand, it is important to emphasize that spontaneous (or therapeutically induced) improvement of ventricular function within a few months of symptom onset is described for 40–50 % of patients and identifies a subgroup with a fair long-term prognosis [70]. Advanced analysis of myocardial tissue samples collected with endomyocardial biopsy is thus far the only way to diagnose the disease definitively and to guide eventual treatment using immunomodulating drugs.

In clinical practice, myocarditis and pericarditis may coexist. This clinical condition is known as perimyocarditis (or myopericarditis) [71]. A precise definition of perimyocarditis is still lacking. Consequently, the true incidence and prevalence of this disease remain unknown. The diagnosis is usually based on the combination of chest pain, pericardial rubs, increased inflammation indexes, electrocardiographic (ECG) and echocardiographic abnormalities (most frequently, pericardial effusion), with troponin release [71]. Clinical presentation is variable and may affect any or all cardiac chambers. Usually, chest pain is the main symptom and is associated with concomitant or recent flu-like syndrome, whereas ventricular/supraventricular arrhythmias and HF with LV dysfunction are rarely observed. Natural history is excellent (survival rate 100 %) during long-term follow-up, regardless of specific etiology and the presence of myocardial involvement (troponin release and WMA at echocardiography) at admission; relapses are relatively infrequent (<10 %) [72].

Typically, patients with myocarditis who present with recent onset of HF demonstrate at echocardiographic study a global impairment of ventricular function without significant remodeling of ventricular chambers, which often maintain a normal or augmented wall thickness and an ellipsoidal shape. Moreover, patchy WMA not corresponding to coronary distribution or ECG changes are often observed (Fig. 21.5, Clips 21.5a and 21.5b) [73, 74]. Additional elements, such as the presence of pericardial effusion, diastolic dysfunction, transient pseudohypertrophy of the ventricular wall, intraventricular thrombi [sometimes multiple and mobile (Fig. 21.6, Clips 21.6a, 21.6b, and 21.6c)] and alteration of the

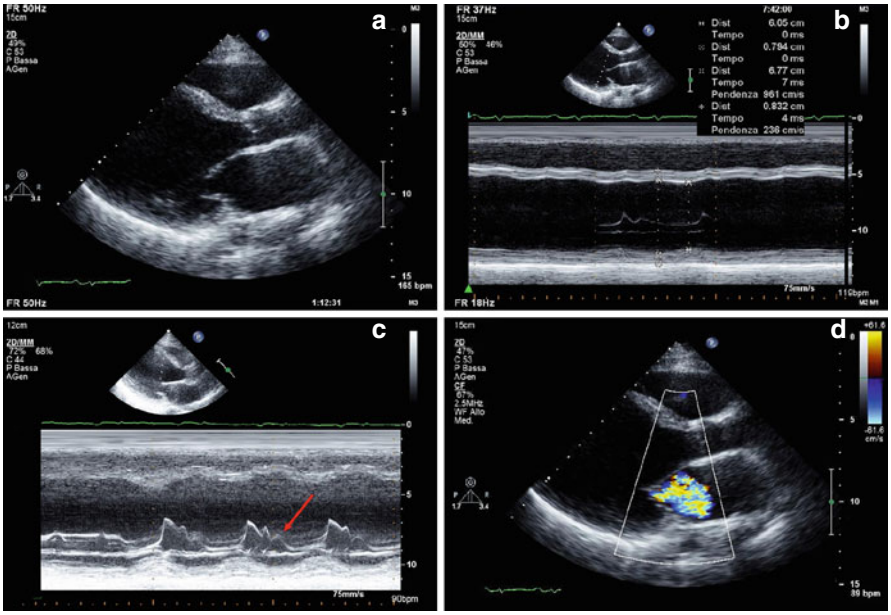

Fig. 21.5 (**a**–**d**) Echocardiographic study in a 33-year-old patient with myocarditis and severe heart failure. Parasternal long-axis view (**a**) and M-mode (**b**) show severe left ventricular (LV) dilation (end-diastolic diameter corrected for body surface area 39 mm/m^2), normal wall thickness, and severe systolic dysfunction (fractional shortening 12 %, ejection fraction 15 %). M-mode recorded at the level of the mitral valve (**c**) shows a B bump (*arrow*), a sign of elevated LV diastolic pressure. Color-Doppler imaging reveals severe functional mitral regurgitation (**d**)

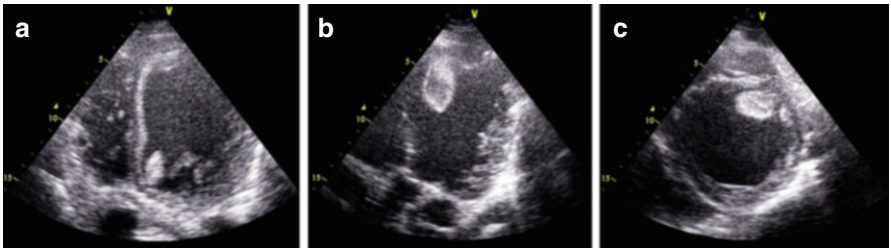

Fig. 21.6 (**a**–**c**) Echocardiogram in a patient with acute myocarditis and severe left ventricular (LV) dysfunction showing multiple pedunculated and mobile thrombi in the LV cavity. Apical four-chamber view (**a**) demonstrating thrombus in the LV attached to the anterior mitral annulus. Apical long-axis view (**b**) showing another pedunculated mobile thrombus attached to the septal apex. Parasternal short-axis view (**c**) in which the apical thrombus is clearly visible

echocardiographic myocardial texture, may further strengthen, if correctly contextualized, the suspicion of myocarditis [73, 75–77]. On the other hand, patients who present with arrhythmias or chest pain and those with perimyocarditis usually exhibit ventricular chambers characterized by normal dimensions, regional wall motion, and global function, even if WMA or transient mild ventricular dysfunction may be observed [72, 78]. In such cases, careful re-evaluation of those

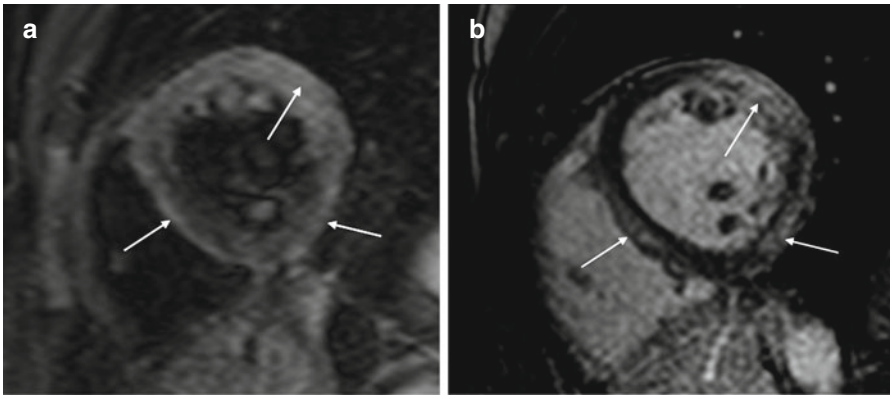

Fig. 21.7 (**a**, **b**) Cardiac magnetic resonance study in acute myocarditis. Midventricular short-axis T2-weighed image (**a**) showing multiple foci of myocardial edema (*arrows*). Midventricular short-axis T1-weighted image after gadolinium contrast administration (**b**) showing late gadolinium enhancement (transmural or subepicardial) in regions corresponding to hyperintensity seen at T2 imaging (*arrows*)

abnormalities with a short-term follow-up is recommended in order to track disease evolution and promptly recognize potentially extensive myocardial involvement.

Recent studies show that LV strain and strain rate may be promising diagnostic parameters in acute myocarditis, even in the presence of normal standard indices, such as LV EF and wall motion. Di Bella et al. [79] demonstrated that strain Doppler echocardiography could detect longitudinal segmental myocardial dysfunction subsequent to myocardial edema in the acute phase of myocarditis.

Further studies using 2D speckle-tracking strain imaging demonstrate that, among all deformation parameters, longitudinal strain appears to be the most powerful index for diagnostic purposes [80, 81]. Furthermore, Escher et al. [82] demonstrated reduced 2D speckle-tracking global systolic longitudinal strain and strain rate in all their patients with biopsy-proven myocarditis (even in those who had preserved LV systolic function); in addition, at follow-up, deformation parameters were significantly lower in patients with than in those without inflammation and correlated significantly with lymphocytic infiltrates. Finally, in a preliminary report, myocardial contrast echocardiography enabled detection of regional perfusion defects that did not conform to a coronary distribution and were not apparent with conventional echocardiography, suggesting the diagnosis of myocarditis later confirmed by CMR [83].

CMR is extensively assessed in scientific literature and is frequently used in clinical practice to evaluate suspected myocarditis [84]. Acute myocarditis, particularly if presenting as acute chest pain and positive markers of myocardial damage without coronary artery disease, frequently has a characteristic pattern at LGE imaging of subepicardial enhancement involving the basal and mid segments of the LV free wall [85] (Fig. 21.7). T2- and T1-weighed early enhancement sequences may, respectively, demonstrate localized myocardial edema and global hyperemia in the inflamed myocardium [86, 87] (Fig. 21.7). The diagnostic accuracy of CMR

compared with the gold-standard of EMB is very high when using a combination of two of the three aforementioned criteria [88].

The same diagnostic criteria were initially reported to have high diagnostic accuracy in cases of myocarditis with clinical presentation such as HF [89]. However, more recent data report limited accuracy when evaluating a single criterion or any combination thereof [90, 91]. These cases are usually characterized by lower-grade diffuse inflammation—which is often impossible to identify with early-enhancement T1- or T2-weighted sequences—and by diffuse interstitial fibrosis, which is missed by LGE sequences [92]. Delayed multidetector CT performed 5 min after contrast injection may be able to identify hyperenhancement similarly to LGE in CMR [93]. This may be a useful alternative in patients with contraindications to CMR.

Echocardiographic recognition of severe myocardial structural derangement with LV enlargement and systolic dysfunction permits identification of patients at risk of major clinical events (death, heart transplantation) in the long-term follow-up. More importantly, data published by our group show that improvement or normalization of LV function at 6 months echocardiographic re-evaluation are associated with a benign long-term prognosis, independently of the pattern of clinical presentation and LV function at presentation [70].

Promising data have been published in recent years on the prognostic role of CMR in the context of myocarditis. The presence of LGE is associated with increased global and arrhythmic cardiac mortality [94]. A pattern of LGE involving the septum, usually from human herpesvirus 6 (HHV6) or combined HHV6 parvovirus B-19 (PVB19) infections, may be predictive of persisting LV dilatation and dysfunction [95].

21.6 Chagas Disease

One peculiar form of myocarditis is Chagas disease, which is caused by *Trypanosoma cruzi*, a flagellated protozoan. This disease continues to represent a health threat for an estimated 28 million people, mostly those living in Latin America [96, 97]. Chagas disease classically presents in an acute or initial phase, which is followed by a chronic phase that can be categorized into indeterminate, cardiac, or digestive forms, each with different clinical manifestations [97]. Severe acute disease is rare (<1 %) and characterized by acute myocarditis, pericardial effusion, and/or meningoencephalitis. After the acute phase, an indeterminate phase usually lasting several years precedes the chronic phase of the disease. The most common and serious problems are cardiac and are caused by an inflammatory CMP as a result of immune reaction and/or the persistence of parasites in the heart. They manifest clinically with progressive HF, life-threatening arrhythmias, and/or thromboembolic events. According to severity of clinical, ECG, chest X-ray, and imaging abnormalities, chronic Chagas CMP is classified into four stages (A, B, C, D) with different mortality and morbidity rates [98]:

- Stage A, or indeterminate, characterized by the absence of symptoms and ECG and structural cardiac abnormalities

- Stage B, with ECG abnormalities (conduction defects and/or arrhythmias) in the absence of symptoms; mild/moderate LV WMA and systolic dysfunction may be present
- Stage C, LV dysfunction at imaging, and prior or current symptoms of HF
- Stage D: symptoms/signs of HF at rest, refractory to medical therapy [New York Heart Association (NYHA) IV]

Most patients affected by Chagas disease have no symptoms for decades after becoming infected with *T. cruzi*. In rare cases, acute myopericarditis can manifest at echocardiography as pericardial effusion, sometimes massive and with tamponade, and/or WMA [97, 99]. In chronic Chagas disease, echocardiographic abnormalities increase in frequency and severity according to the clinical stage of the disease [97, 99, 100]. The typical, although not pathognomonic, pattern is the presence of apical LV aneurysm, with or without global chamber dilatation and depressed systolic function (Clips 21.7a, 21.7b, 21.7c, and 21.7d) [99, 100]. Diastolic dysfunction is an important hallmark of Chagas disease and usually precedes systolic dysfunction [97]. Also, RV involvement is a typical feature of the disease and is usually associated with LV dysfunction; occasionally a RV apical aneurysm is observed [97]. Patients with LV aneurysms, similarly to those with this complication of myocardial infarction, are at risk of thrombosis and systemic embolism.

Few data are available regarding the usefulness of new echocardiographic techniques in Chagas disease. Tissue-Doppler-imaging (TDI) derived myocardial strain can demonstrate lower radial and longitudinal values compared with normal individuals and could quantify subtle segmental contractile dysfunction not detected visually [99]. Speckle-tracking technology is used to quantify global and segmental LV deformation (radial, circumferential, and longitudinal strain) and twist and untwisting velocities [101]. In that study, global strains showed a significant decreasing trend across groups of disease severity. Interestingly, patients in the indeterminate form had significantly lower radial strains in both the global and midinferior segment and lower twist and untwisting velocities compared with normal individuals. CMR may help in diagnosing Chagas CMP by demonstrating aneurysm formation with preferential sites at the apex and inferolateral walls. Aneurysms are easily detected with SSFP cine imaging. The pattern of LGE is variable and may involve any or all layers of the myocardial wall [102, 103].

Prognosis in Chagas disease mainly depends on the clinical stage of the disease [97]. No mortality is reported for patients in the indeterminate phase. In one series of 843 initially asymptomatic patients with Chagas disease [100], during long-term follow-up (mean 9.9 ± 5.3 years), a change in clinical stage, LV systolic dimension at M-mode echocardiography, and EF were the only independent predictors of mortality. The frequency and severity of echocardiographic abnormalities increases with increasing severity of disease stage. In that series, mortality and event rates were, respectively, 0 and 8 % of 505 patients in group 0; 1 and 26 % of 257 patients of group 1; and 14 and 52 % of 87 patients of group 2.

Nunes et al. [104] reported on the prognostic value of LA volume assessed by 2D echocardiography, adding incremental prognostic value to clinical factors (NYHA class), LV EF, RV function, and Doppler parameters of diastolic function [Ratio of

transmitral E velocity to mitral annular E′ velocity (E/E′)]. In that series, an LA-indexed end-systolic volume >51 ml/m^2 was associated with significant excess mortality. The prognostic impact of TDI index on LV diastolic dysfunction (E/E′) was subsequently analyzed by Nunes et al. [105], who showed a different and opposite prognostic significance of E/E′ according to LV systolic dysfunction severity. In fact, a high E/E′ (>15) was a strong adverse prognostic factor only for patients with mild to moderate LV EF depression (>30 %), whereas it was "protective" in the subset patients with severe LV systolic dysfunction. An interaction between RV dysfunction, frequent in the most severe cases with advanced congestive HF, was hypothesized.

21.7 Chemotherapy-Induced Cardiomyopathy

The incidence of complications after antineoplastic therapy is increasing in relation to the incidence of cancer and prolonged survival rate. Cardiotoxicity is one of the major complications. The Cardiac Review and Evaluation Committee established some criteria for diagnosing chemotherapy-related cardiac dysfunction [106], which consider clinical history, LV EF reduction, and presence of HF symptoms and signs. Echocardiography is recommended before the start of treatment and periodically during and after chemotherapy cycles. Anthracyclines (doxorubicin, daunomycin, idarubicin) are the most frequent chemotherapeutic agents involved in cardiotoxicity; however, adverse cardiotoxic effects are reported also for other drugs (mitoxantrone, 5-fluorouracil, cyclophosphamide, trastuzumab). Anthracycline may exhibit two different types of cardiac toxicity over time: early-onset cardiotoxicity (often expressed with ventricular or supraventricular arrhythmias), or late-onset chronic cardiotoxicity that emerges many years after chemotherapy has been completed. The risk and severity of anthracycline CMP is typically dose related. Clinical manifestations are those of severe biventricular HF with decreased EF and frequently severe diastolic dysfunction. Because of the progressive morphologic changes and the persistence of changes over a long period, symptoms are reported to occur any time up to months after stopping the drug. Although HF is reported to have a high mortality rate, successful treatment is possible [107].

Traditional therapies, such as anthracyclines, have been recognized for years as causing cardiovascular complications. Less expected were the cardiovascular effects of targeted cancer therapies, which were initially thought to be specific to cancer cells and would spare any adverse effects on the heart. In patients with breast cancer treated with anthracyclines, taxanes, and trastuzumab, systolic longitudinal myocardial strain and ultrasensitive troponin I measured at the completion of anthracycline therapy are useful for predicting subsequent cardiotoxicity and may help guide treatment [108].

Echocardiographic characteristics of anthracyclines-induced CMP are indistinguishable from other causes of LV dysfunction [109]. A typical pattern is a mildly dilated but severely dysfunctioning LV with severe diastolic dysfunction [restrictive

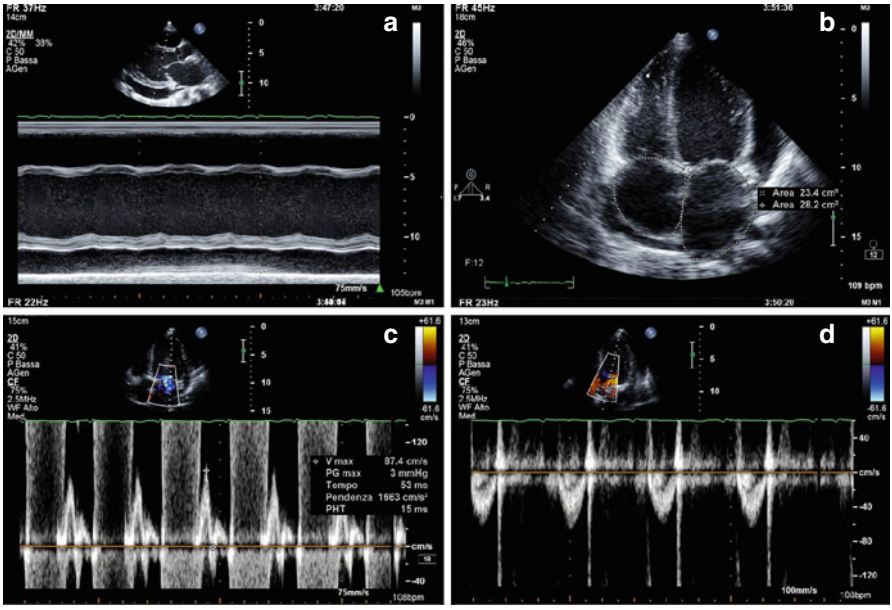

Fig. 21.8 (**a**–**d**) A 19-year-old patient with cardiomyopathy that developed after chemiotherapy (including anthracyclines) and radiotherapy for acute lymphatic leukemia. M-mode echocardiography (**a**), parasternal long-axis view, shows moderate left ventricular (LV) dilation (end-diastolic diameter corrected for body surface area 36 mm/mq), with severe systolic dysfunction (fractional shortening 11 %). There is also pericardial effusion posteriorly to the LV (21-mm thick), around the right atrium (12 mm), and laterally to the LV (14 mm), as shown in the apical four-chamber view (**b**), which also shows mild biatrial dilation. Pulsed-wave-Doppler interrogation of transmitral flow reveals a restrictive filling pattern (**c**). Pulsed-wave Doppler of the aortic valve (**d**) shows a low velocity (0.5 m/s), a sign of low cardiac output

filling pattern (RFP)}. RV dysfunction, MR, tricuspid regurgitation (TR), and pulmonary hypertension are frequently present (Fig. 21.8, Clips 21.8a, 21.8b, 21.8c, and 21.8d). Other antineoplastic drugs, such as the monoclonal antibody trastuzumab, can induce reversible forms of cardiac dysfunction [110].

Furthermore, several forms of cancer treatment, such as 5-fluorouracil, are associated with an increased risk of coronary artery disease and/or acute coronary syndrome, with transient regional hypokinesia at echocardiographic evaluation.

Strain and strain-rate imaging is used to detect subtle early impairment in cardiac contractility due to chemotherapeutic agents. Reduced strain and strain-rate parameters can, in fact, precede any appreciable change in LV EF and might therefore help in identifying patients who develop chemotherapy-related cardiotoxicity in an early subclinical stage (Fig. 21.9) [111]. Early subclinical abnormalities occur after low to moderate dosages of anthracycline-based chemotherapy and persist after 6 months, although without evidence of myocardial fibrosis by LGE [112].

CMR is able to detect significantly reduced LV EF and cardiac mass in survivors of childhood cancer previously undiagnosed with cardiotoxicity by 2D

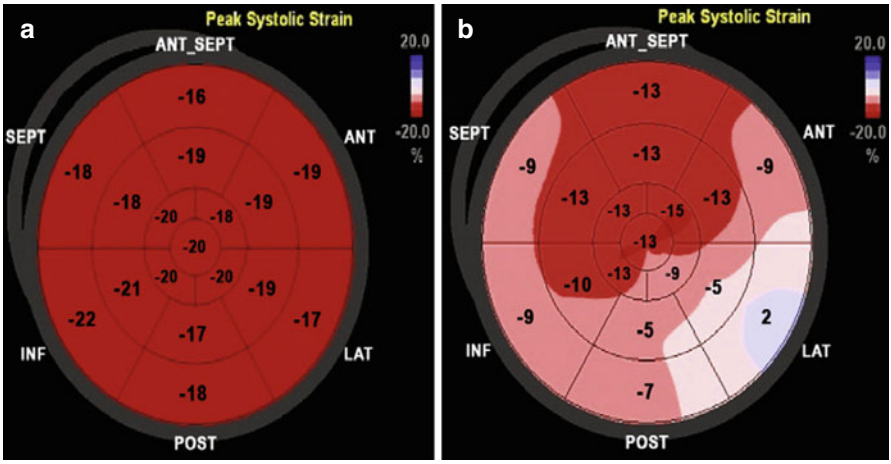

Fig. 21.9 (**a**, **b**) Normal 2D global longitudinal strain (−19.5 %) (**a**) measured in a 22-year-old woman before chemotherapy treatment. After 6 months of chemotherapy (**b**), a significant reduction in global longitudinal strain is observed (−10.1 %) despite persistence of normal left ventricular ejection fraction. *ANT* anterior, *ANT_SEPT* anteroseptal, *INF* inferior, *LAT* lateral, *POST* posterior, *SEPT* septal (From Oreto et al. [111], with permission)

echocardiography [113, 114]. Indexed LV mass by CMR is inversely associated with cumulative anthracycline dose and predictive of events at follow-up [115]; LGE is rare [114, 115]. Diffuse myocardial fibrosis seen at T1 mapping may represent an early marker of anthracycline cardiotoxicity [116, 117].

Conversely, when trastuzumab is combined with anthracyclines for human epidermal growth factor receptor-2 (HER-2)-positive breast cancer, subepicardial lateral wall LGE is often found in patients who develop drug-induced CMP [118]. Serial LV EF determination may be performed using ^{99m}Tc radionuclide ventriculography and has long been regarded as the gold standard for measuring anthracycline cardiotoxicity in adult patients [119]. Imaging with [^{123}I]-MIBG or ^{123}I-labelled antimyosin may detect subclinical changes before LV function is impaired in patients treated with anthracyclines [120].

Regular heart-function monitoring during treatment is important to detect cardiac involvement in neoplastic patients treated with chemotherapy. A baseline, LV EF evaluation is usually necessary. It is recommended that the same methodology be used for comparing serial studies [109]. Decreased longitudinal strain, together with troponin I, increases early after treatment with anthracyclines and trastuzumab, can predict cardiotoxicity development [108]. CMR imaging is also emerging as a promising tool in the oncology setting [113].

A clinically important deterioration in LV function can be variously defined (i.e., 10 % absolute decrease in LV fractional shortening, 10 % decrease in LV EF, or absolute LV EF value <55 %). Guidelines recommend discontinuing anthracycline therapy if LV deterioration is found and, preferably, is confirmed on two successive tests [110].

Treating anthracycline-induced LV dysfunction is the same as for treating other causes of myocardial dysfunction according to international HF guidelines. Echocardiography continues to be the mainstay of monitoring therapeutic efficacy, given that it is portable, widely available, noninvasive, causes minimal pain, and provides real-time data [110].

21.8 Left Ventricular Noncompaction

A position statement from the European Society of Cardiology categorized LV NC as an "unclassified CMP," asserting: "it is not clear whether it is a separate cardiomyopathy or merely a morphological trait shared by many phenotypically distinct cardiomyopathies" [121]. There is no gold-standard criteria for making this diagnosis, so that it can even be difficult to assess the real incidence of the disease. In 1990, Chin et al. [122] proposed echocardiographic criteria for diagnosing this entity. LV NC can be present from birth or it can develop later in life. It is difficult to identify strong predictors of outcome to select effective management strategies in this CMP due to the rarity of the disease and to different studies that are not comparable for type and number of patients included [123]. The standard therapy HF management should be applied to patients with LV NC and LV dysfunction.

Systemic thromboembolic events are commonly associated with LV NC. However, there is no agreement in the cardiology community regarding the use warfarin and/or antiplatelet therapy, particularly in patients with preserved LV EF, and the risk/benefit ratio must be individualized. Also the practice to use anticoagulation in patients with LV NC and significantly impaired LVEF is not based on robust data [124].

The typical echocardiographic features of LV NC are the presence of multiple, prominent LV endocardial trabeculations separated by multiple, deep intertrabecular recesses filled with blood from the ventricular cavity, with a predominant involvement of the apex, the lateral, and the inferior wall. Wall thickness of spared segments is normal [123]. Dimensions and shape of cardiac chambers are usually preserved [122], but, in the late stages of HF, the LV can also be significantly dilated. Noncompacted segments are usually hypokinetic, such as the noninvolved walls; therefore, the LV systolic function is commonly depressed (~60 % of patients). Maximal end-systolic ratio of the noncompacted endocardial layer to the compacted myocardium and the number of affected segments are independent predictors of LV systolic dysfunction [125].

RV involvement is reported in 20–30 % of cases [126], but it is very difficult to demonstrate due to the normal trabeculated pattern of the RV walls. Myocardial thickness is apparently increased, but with a patchy structure and deep intertrabecular recesses, which are radially oriented. Usually, these aspects are better appreciated in childhood (Fig. 21.10, Clips 21.9a and 21.9b). Considering its predominant direction, anomalous trabeculation should be assessed by multiple views. Oblique of-axis images or images in the parasternal short-axis view, which are not perpendicular to the LV long axis, can produce the morphological appearance of prominent

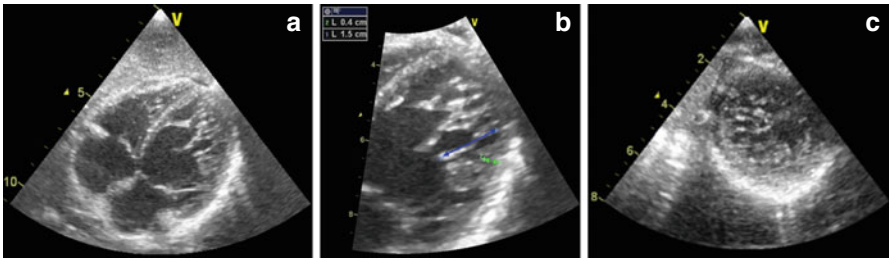

Fig. 21.10 (**a**–**c**) Echocardiographic study in a 6-year-old patient with left ventricular (LV) noncompaction. Subcostal four-chamber view (**a**) showing multiple endocardial trabeculations in the LV lateral wall, with normal wall thickness of the spared segments. Compacted myocardium thickness is 4 mm (*green arrow*); compacted + noncompacted myocardial thickness is 15 mm at end-diastole (*blue arrow*) (**b**). Subcostal short-axis view (**c**) showing the typical honeycomb appearance

trabeculations and thus mimic LV NC. It is therefore crucial to obtain images that are not foreshortened and are perpendicular to the ventricular long axis [124]. Color-Doppler flow imaging can be useful to detect intertrabecular recesses filled with blood in the LV cavity. In adults, prominent trabeculations are less evident; more frequently, there are echo-free spaces interrupting the homogeneous myocardial echogenic pattern [127]. Moreover, typically, progressive increase in the noncompacted/compacted segment ratio from base to apex is seen, showing the typical honeycomb appearance [128]. The presence of thrombi, which are hidden in the sponge-like myocardium, can be detected by 2D echocardiography, but the accuracy of CMR is certainly superior. Diastolic function is usually affected, and an restrictive pattern is present in 20–40 % of patients [126]. Atrial cavities are typically dilated [127]. Differential diagnosis can be challenging and includes apical form of HCM, a combination of apical HCM and LV NC, hypertensive CMP, endocardial fibroelastosis, abnormal chords, apical thrombus, or tumors [129]. Differential diagnosis between DCM and LV NC can be a challenge, especially in dilated ventricles. Furthermore, the degree of trabeculated LV myocardium is far more frequent than previously thought; this supports the concept of a continuous trait between the normal and pathological appearance of the myocardium [130]. Given the high interobserver variability, it is not sufficient to limit the diagnostic approach to a simple qualitative morphologic assessment. Therefore, three different quantitative diagnostic criteria exist (Table 21.1). All criteria are based on morphological findings and require the presence of prominent trabeculations, with deep intertrabecular recesses communicating with the ventricular cavity, as well as a two-layered appearance of the myocardium (trabecular myocardium as one layer, compacted myocardium as the second layer) [122, 131–134]. Chin et al. [122] calculated the ratio between the depth of the intertrabecular recesses and posterior wall thickness by comparing the distance between the epicardial surface trough of intertrabecular recesses (*X*) with the distance between the epicardial surface and peak trabeculations (*Y*) in end-diastole. A decade later, Jenni et al. [131] published their criteria for LV NC consisting of four components and validated with anatomical heart preparations. In contrast to

Table 21.1 Echocardiographic diagnostic criteria for left ventricular noncompaction (LV NC)

Study	Criteria
Chin et al. [122]	Two-layered structure of the myocardium (epicardial compacted, endocardial noncompacted layer) Determination of *X* to *Y* ratio (≤0.5). *X*: distance between epicardial surface and through intertrabecular recess; *Y*: distance between epicardial surface and peak of trabeculation Image acquisition. Parasternal short-axis view, measurements of *X* to *Y* ratio at end-diastole
Jenni et al. [127, 131]	Image acquisition. Short-axis views, measurement of noncompacted (N)/compacted (C) ratio at end-systole Thickened myocardium, with a two-layered structure consisting of a thin, compacted, epicardial layer/band (C) and a much thicker, noncompacted, endocardial layer (N) or trabecular meshwork with deep endomyocardial spaces; N/C ratio >2.0 Predominant location of the pathology. Midlateral, midinferior, and apex Color-Doppler evidence of deep intertrabecular recesses filled with blood from the left ventricular cavity Absence of coexisting cardiac abnormalities (in the presence of isolated LV NC)
Stollberger et al. [132, 133]	More than three trabeculations protruding from the LV wall, located apically to the papillary muscles and visible in one image plane Trabeculations with the same echogenicity as the myocardium and synchronous movement with ventricular contractions. Perfusion of intertrabecular spaces from the LV cavity Ratio of noncompacted to compacted segment >2.0 at end-diastole (this criterion was introduced later) Image acquisition. Apical four-chamber view; transducer angulation, and image acquisition in atypical views to obtain the best technical picture quality for differentiation between false chords/aberrant bands and trabeculations Diagnostic criteria have changed in recent years

Chin et al., the Zurich group relied on measurements at end-systole because the thickness of the two layers is best visualized in that phase. The combination of these criteria was very specific [135]. The third criteria, by Stollberger et al. [132], required the presence of more than three trabeculations located apical to insertion of the papillary muscles, as visible in one apical image plane. These authors were the first to clearly define trabeculations as structures with the same echogenicity as the myocardium, moving synchronously with the ventricle.

Belanger et al. [136] also assessed the utility of the LV trabecular area as measured by echocardiography using a four-chamber view to identify LV NC.

Several limitations are reported regarding these criteria. Kohli et al. [137] demonstrated an unexpectedly high percentage (23.6 %) of patients with HF fulfilling one or more of the diagnostic criteria for LV NC, in addition to 8.3 % of healthy controls. Furthermore, the reproducibility of the measurement of noncompacted/compacted segment ratio, such as the quantification of trabeculations, has been shown to be poor [138]. Interestingly, a high proportion of young athletes (8.1 %) fulfilled conventional criteria for LV NC [139].

When noncompaction is subtle or incomplete, differential diagnosis with other disorders is uncertain. Contrast echocardiography can be helpful in such cases or

when conventional echocardiographic images are poor, improving visualization of trabeculations and the compacted myocardium, and illustrating intertrabecular perfusion [140]. Moreover, TEE can support the diagnosis of LV NC, thus highlighting the spongy appearance of the LV walls and showing the peculiar morphology of the papillary muscles [141]. Finally, it can be helpful when intraventricular thrombi cannot be excluded by TTE.

A functional evaluation, in addition to morphological assessment, can be useful in LV NC diagnosis. Myocardial strain values are abnormal in patients with LV NC, even in the context of preserved systolic function [142]. In addition, an abnormal pattern of LV twist/rotation was observed on speckle-tracking echocardiography in patients with LV NC. In one study [143], rotation was clockwise at the base and counterclockwise at the apex in all controls as well as in patients with DCM. In contrast, LV base and apex rotated in the same direction (LV solid-body rotation) in all LV NC patients. Thus, LV solid-body rotation/twist may be a new objective, functional, and quantitative diagnostic criterion for this CMP. However, this feature might not be entirely specific [144] and was not present in all LV NC patients in another study [145]. In that study, the presence of rigid-body rotation was not associated with worse LV remodelling compared with LV NC individuals with normal twist.

Furthermore, Nieman et al. [146] found no difference in standard echocardiographic parameters between LV NC and DCM but observed a unique regional deformation pattern in LV NC characterized by preserved deformation in basal segments with decreased myocardial deformation in more apical segments. Conversely, in DCM, strain and strain rate were homogeneously reduced in all LV segments. Thus, the authors proposed this special regional deformation pattern as an additional diagnostic tool to differentiate LV NC from DCM (Fig. 21.11).

In LV NC, 3D echocardiography allows a more comprehensive LV assessment, including trabecular volume measurement, which may further aid in diagnosis (Fig. 21.12) [147]. Moreover, Bodiwala et al. [148] suggested the use of 3D echocardiography to visualize the trabecular meshwork, referred to as a honeycomb appearance, as an useful feature for differentiating LV NC from other diseases.

CMR has an important diagnostic contribution in suspected LV NC, particularly in patients with poor echocardiographic quality. A ratio between noncompacted and compacted myocardium >2.3:1 seen at steady-state free-precession (SSFP) CMR sequences was demonstrated to have high sensitivity and specificity and is the accepted diagnostic criterion for diagnosing this disease [149] (Fig. 21.13). However, when using this criterion, an unexpectedly high rate of LV NC is found [150]. Other proposed diagnostic criteria are the percentage of LV trabeculated mass >20 % [151, 152] or >25 %, or >15 g/m^2 indexed noncompacted myocardial mass [153]. Operators must be aware of the potential pitfalls in CMR, which have frequently led to overdiagnosis of LV NC, such as assessing long-axis instead of short-axis views [150], possibly due to incorrect piloting of long-axis planes [154].

LGE correlates with the extent of WMA and severity of clinical status [155–157]. However, these relations were not confirmed in other series [153, 158].

Multidetector CT (MDCT) of the heart may be a valuable diagnostic option. A noncompacted to compacted ratio of 2.2 or 2.3 measured in end-diastole, and involvement of two or more segments, is suggested to distinguish LV NC from other CMP and healthy individuals [159, 160].

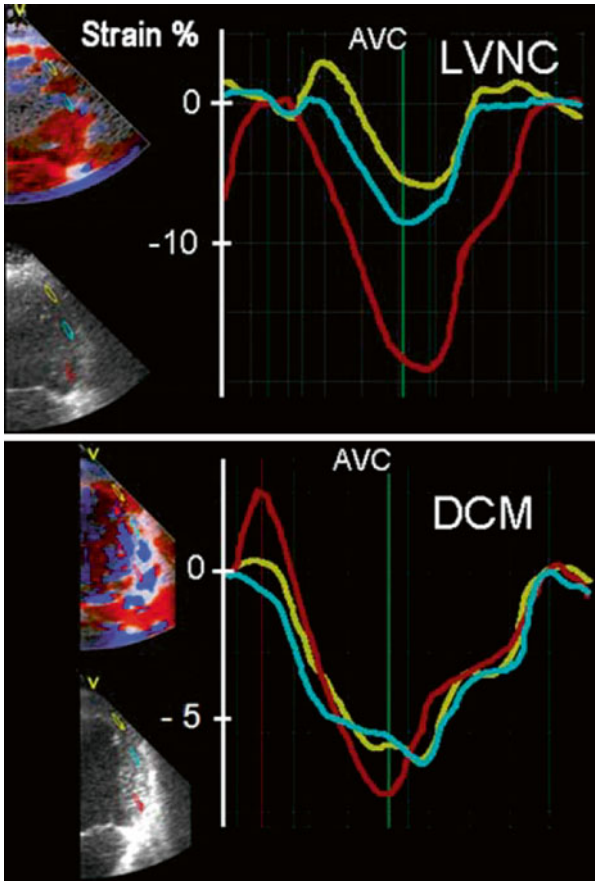

Fig. 21.11 Tissue-Doppler strain imaging performed in three lateral wall segments in a patient with left ventriculare noncompaction (*LV NC*) (*upper*) and dilated cardiomyopathy (*DCM*) (*lower*). *Yellow*, *blue*, and *red curves* show strain curves in apical, mid, and basal segments, respectively. There is an increasing gradient in end-systolic strain from the apex to the base in the patient with LV NC, whereas strain in the patient with DCM is homogeneously reduced. *AVC* aortic valve closure (From Niemann et al. [146], with permission)

Regional myocardial perfusion defects assessed by [^{13}N]-ammonia PET are described in most noncompacted segments and in a minority of normal segments. Coronary flow reserve is significantly decreased in most segments with WMA and not confined to noncompacted segments only [161].

Considering the possible prognostic implications of imaging, the presence of LV systolic dysfunction in LV NC is related with the number of affected segments and the thickness of the noncompacted layer [125]. LV dysfunction by itself places patients at a higher risk for morbidity and mortality [162]. Other echocardiographic predictors of adverse outcome are reported in previous studies, specifically the ratio of noncompacted to compacted layers, the number of affected segments, the LV end-diastolic diameter, and an a decreased E′ velocity of the LV lateral wall on TDI [123, 125, 163–165].

Patients with systolic dysfunction, even if asymptomatic, should be treated with evidenced-based HF therapy and need careful follow-up. Insertion of an implantable cardioverter defibrillator (ICD) for primary prevention should be considered, according to guidelines, for nonischemic CMP [166].

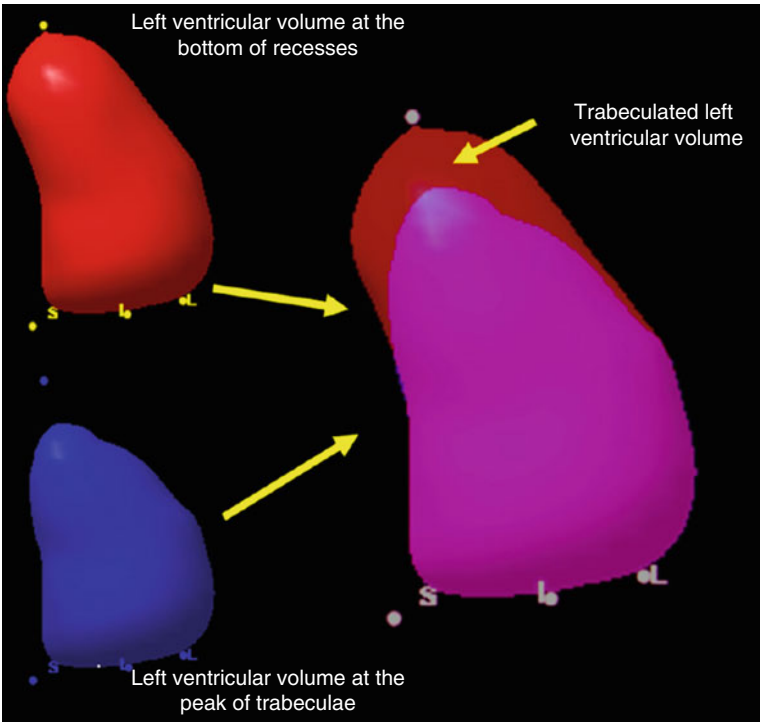

Fig. 21.12 Result of the 3Dechocardiographic analysis for trabeculated left ventricular (LV) volume estimation in a patient with LV noncompaction. After tracing the endocardial border at the bottom of the trabeculae and at the peak of the recesses, end-diastolic volumes including (*red*) and excluding (*blue*) trabeculae are obtained. Yellow arrows indicate that the difference between volumes (*blue* and *red*) corresponds to the trabeculated LV volume (indicated by the other yellow arrow), which is normalized by LV end-diastolic volume including trabeculae and represents the proportion of the LV cavity occupied by trabeculae (From Caselli et al. [147], with permission)

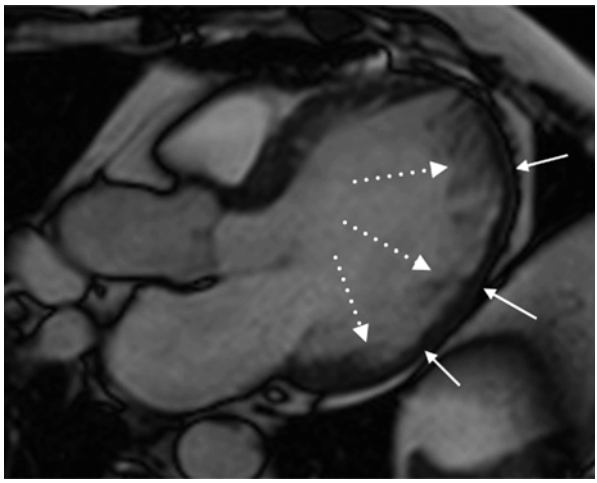

Fig. 21.13 Patient with left ventricular noncompaction (LV NC). Steady-state free-precession cardiac magnetic resonance, three-chamber image, taken at end-diastole showing a thick layer of noncompacted myocardium (*dotted arrows*) over compacted myocardium (*solid arrows*) in LV posterior wall

References

1. Huffman C, Wagman G, Fudim M et al (2010) Reversible cardiomyopathies – a review. Transplant Proc 42:3673–3678
2. Demakis JG, Rahimtoola SH, Sutton GC et al (1971) Natural course of peripartum cardiomyopathy. Circulation 44:1053–1061
3. Pearson GD, Veille JC, Rahimtoola S et al (2000) Peripartum cardiomyopathy: National Heart, Lung, and Blood Institute and Office of Rare Diseases (National Institutes of Health) workshop recommendations and review. JAMA 283:1183–1188
4. Givertz MM (2013) Cardiology patient page: peripartum cardiomyopathy. Circulation 127:e622–e626
5. Sliwa K, Skudicky D, Bergemann A et al (2000) Peripartum cardiomyopathy: analysis of clinical outcome, left ventricular function, plasma levels of cytokines and Fas/APO-1. J Am Coll Cardiol 35:701–705
6. Bello N, Rendon IS, Arany Z (2013) The relationship between pre-eclampsia and peripartum cardiomyopathy: a systematic review and meta-analysis. J Am Coll Cardiol 62:1715–1723
7. Peters F, Khandheria BK, dos Santos C et al (2013) Peripartum cardiomyopathy associated with left ventricular noncompaction phenotype and reversible rigid body rotation. Circ Heart Fail 6:e62–e63
8. Renz DM, Rottgen R, Habedank D et al (2011) New insights into peripartum cardiomyopathy using cardiac magnetic resonance imaging. Röfo 183:834–841
9. Arora NP, Mohamad T, Mahajan N et al (2014) Cardiac magnetic resonance imaging in peripartum cardiomyopathy: a new tool to evaluate an old enigma. Am J Med 347:112–7.
10. Blauwet LA, Libhaber E, Forster O et al (2013) Predictors of outcome in 176 South African patients with peripartum cardiomyopathy. Heart 99:308–313
11. Dorbala S, Brozena S, Zeb S et al (2005) Risk stratification of women with peripartum cardiomyopathy at initial presentation: a dobutamine stress echocardiography study. J Am Soc Echocardiogr 18:45–48
12. Maron BJ, Towbin JA, Thiene G et al (2006) Contemporary definitions and classification of the cardiomyopathies: an American Heart Association Scientific Statement from the Council on Clinical Cardiology, Heart Failure and Transplantation Committee; Quality of Care and Outcomes Research and Functional Genomics and Translational Biology Interdisciplinary Working Groups; and Council on Epidemiology and Prevention. Circulation 113:1807–1816
13. Bybee KA, Kara T, Prasad A et al (2004) Systematic review: transient left ventricular apical ballooning: a syndrome that mimics ST-segment elevation myocardial infarction. Ann Intern Med 141:858–865
14. Ruiz Bailen M, Aguayo de Hoyos E, Lopez Martnez A et al (2003) Reversible myocardial dysfunction, a possible complication in critically ill patients without heart disease. J Crit Care 18:245–252
15. Kawai S, Kitabatake A, Tomoike H et al (2007) Guidelines for diagnosis of takotsubo (ampulla) cardiomyopathy. Circ J 71:990–992
16. Lyon AR, Rees PS, Prasad S et al (2008) Stress (Takotsubo) cardiomyopathy – a novel pathophysiological hypothesis to explain catecholamine-induced acute myocardial stunning. Nat Clin Pract Cardiovasc Med 5:22–29
17. Lee JW, Kim JY (2011) Stress-induced cardiomyopathy: the role of echocardiography. J Cardiovasc Ultrasound 19:7–12
18. Kurisu S, Kihara Y (2012) Tako-tsubo cardiomyopathy: clinical presentation and underlying mechanism. J Cardiol 60:429–437
19. Ramaraj R, Movahed MR (2010) Reverse or inverted takotsubo cardiomyopathy (reverse left ventricular apical ballooning syndrome) presents at a younger age compared with the mid or apical variant and is always associated with triggering stress. Congest Heart Fail 16:284–286
20. Kurisu S, Inoue I, Kawagoe T et al (2011) Incidence and treatment of left ventricular apical thrombosis in Tako-tsubo cardiomyopathy. Int J Cardiol 146:e58–e60

21. Gianni M, Dentali F, Grandi AM et al (2006) Apical ballooning syndrome or takotsubo cardiomyopathy: a systematic review. Eur Heart J 27:1523–1529
22. Izumo M, Nalawadi S, Shiota M et al (2011) Mechanisms of acute mitral regurgitation in patients with takotsubo cardiomyopathy: an echocardiographic study. Circ Cardiovasc Imaging 4:392–398
23. Elesber AA, Prasad A, Bybee KA et al (2006) Transient cardiac apical ballooning syndrome: prevalence and clinical implications of right ventricular involvement. J Am Coll Cardiol 47:1082–1083
24. Kumar S, Kaushik S, Nautiyal A et al (2011) Cardiac rupture in takotsubo cardiomyopathy: a systematic review. Clin Cardiol 34:672–676
25. Shah BN, Simpson IA, Rakhit DJ (2011) Takotsubo (apical ballooning) syndrome in the recovery period following dobutamine stress echocardiography: a first report. Eur J Echocardiogr 12:E5
26. Choi JH, Nam JH, Son JW et al (2012) Clinical usefulness of myocardial contrast echocardiography to detect stress-induced cardiomyopathy in the emergency department. Circ J 76:1393–1398
27. Meimoun P, Malaquin D, Benali T et al (2009) Transient impairment of coronary flow reserve in tako-tsubo cardiomyopathy is related to left ventricular systolic parameters. Eur J Echocardiogr 10:265–270
28. Abdel-Aty H, Cocker M, Friedrich MG (2009) Myocardial edema is a feature of Tako-Tsubo cardiomyopathy and is related to the severity of systolic dysfunction: insights from T2-weighted cardiovascular magnetic resonance. Int J Cardiol 132:291–293
29. Joshi SB, Chao T, Herzka DA et al (2010) Cardiovascular magnetic resonance T2 signal abnormalities in left ventricular ballooning syndrome. Int J Cardiovasc Imaging 26:227–232
30. Neil C, Nguyen TH, Kucia A et al (2012) Slowly resolving global myocardial inflammation/oedema in Tako-Tsubo cardiomyopathy: evidence from T2-weighted cardiac MRI. Heart 98:1278–1284
31. Eitel I, Lucke C, Grothoff M et al (2010) Inflammation in takotsubo cardiomyopathy: insights from cardiovascular magnetic resonance imaging. Eur Radiol 20:422–431
32. Ferreira VM, Piechnik SK, Dall'Armellina E et al (2012) Noncontrast T1-mapping detects acute myocardial edema with high diagnostic accuracy: a comparison to T2-weighted cardiovascular magnetic resonance. J Cardiovasc Magn Reson 14:42
33. Gerbaud E, Montaudon M, Leroux L et al (2008) MRI for the diagnosis of left ventricular apical ballooning syndrome (LVABS). Eur Radiol 18:947–954
34. Mitchell JH, Hadden TB, Wilson JM et al (2007) Clinical features and usefulness of cardiac magnetic resonance imaging in assessing myocardial viability and prognosis in Takotsubo cardiomyopathy (transient left ventricular apical ballooning syndrome). Am J Cardiol 100:296–301
35. Eitel I, Behrendt F, Schindler K et al (2008) Differential diagnosis of suspected apical ballooning syndrome using contrast-enhanced magnetic resonance imaging. Eur Heart J 29:2651–2659
36. Eitel I, von Knobelsdorff-Brenkenhoff F, Bernhardt P et al (2011) Clinical characteristics and cardiovascular magnetic resonance findings in stress (takotsubo) cardiomyopathy. JAMA 306:277–286
37. Nakamori S, Matsuoka K, Onishi K et al (2012) Prevalence and signal characteristics of late gadolinium enhancement on contrast-enhanced magnetic resonance imaging in patients with takotsubo cardiomyopathy. Circ J 76:914–921
38. Naruse Y, Sato A, Kasahara K et al (2011) The clinical impact of late gadolinium enhancement in Takotsubo cardiomyopathy: serial analysis of cardiovascular magnetic resonance images. J Cardiovasc Magn Reson 13:67
39. Ito K, Sugihara H, Kawasaki T et al (2001) Assessment of ampulla (Takotsubo) cardiomyopathy with coronary angiography, two-dimensional echocardiography and 99mTc-tetrofosmin myocardial single photon emission computed tomography. Ann Nucl Med 15:351–355

40. Abe Y, Kondo M, Matsuoka R et al (2003) Assessment of clinical features in transient left ventricular apical ballooning. J Am Coll Cardiol 41:737–742
41. Ito K, Sugihara H, Katoh S et al (2003) Assessment of Takotsubo (ampulla) cardiomyopathy using 99mTc-tetrofosmin myocardial SPECT – comparison with acute coronary syndrome. Ann Nucl Med 17:115–122
42. Kurisu S, Inoue I, Kawagoe T et al (2003) Myocardial perfusion and fatty acid metabolism in patients with tako-tsubo-like left ventricular dysfunction. J Am Coll Cardiol 41:743–748
43. Owa M, Aizawa K, Urasawa N et al (2001) Emotional stress-induced 'ampulla cardiomyopathy': discrepancy between the metabolic and sympathetic innervation imaging performed during the recovery course. Jpn Circ J 65:349–352
44. Sato A, Aonuma K, Nozato T et al (2008) Stunned myocardium in transient left ventricular apical ballooning: a serial study of dual I-123 BMIPP and Tl-201 SPECT. J Nucl Cardiol 15:671–679
45. Pessoa PM, Xavier SS, Lima SL et al (2006) Assessment of takotsubo (ampulla) cardiomyopathy using iodine-123 metaiodobenzylguanidine scintigraphy. Acta Radiol 47:1029–1035
46. Cimarelli S, Sauer F, Morel O et al (2010) Transient left ventricular dysfunction syndrome: patho-physiological bases through nuclear medicine imaging. Int J Cardiol 144:212–218
47. Burgdorf C, von Hof K, Schunkert H et al (2008) Regional alterations in myocardial sympathetic innervation in patients with transient left-ventricular apical ballooning (Tako-Tsubo cardiomyopathy). J Nucl Cardiol 15:65–72
48. Bybee KA, Murphy J, Prasad A et al (2006) Acute impairment of regional myocardial glucose uptake in the apical ballooning (takotsubo) syndrome. J Nucl Cardiol 13:244–250
49. Feola M, Chauvie S, Rosso GL et al (2008) Reversible impairment of coronary flow reserve in takotsubo cardiomyopathy: a myocardial PET study. J Nucl Cardiol 15:811–817
50. Yoshida T, Hibino T, Kako N et al (2007) A pathophysiologic study of tako-tsubo cardiomyopathy with F-18 fluorodeoxyglucose positron emission tomography. Eur Heart J 28:2598–2604
51. Kwon SW, Kim BO, Kim MH et al (2013) Diverse left ventricular morphology and predictors of short-term outcome in patients with stress-induced cardiomyopathy. Int J Cardiol 168:331–337
52. Lee PH, Song JK, Sun BJ et al (2010) Outcomes of patients with stress-induced cardiomyopathy diagnosed by echocardiography in a tertiary referral hospital. J Am Soc Echocardiogr 23:766–771
53. Elesber AA, Prasad A, Lennon RJ et al (2007) Four-year recurrence rate and prognosis of the apical ballooning syndrome. J Am Coll Cardiol 50:448–452
54. Ellis ER, Josephson ME (2013) Heart failure and tachycardia-induced cardiomyopathy. Curr Heart Fail Rep 10:296–306
55. Jeong YH, Choi KJ, Song JM et al (2008) Diagnostic approach and treatment strategy in tachycardia-induced cardiomyopathy. Clin Cardiol 31:172–178
56. Fujino T, Yamashita T, Suzuki S et al (2007) Characteristics of congestive heart failure accompanied by atrial fibrillation with special reference to tachycardia-induced cardiomyopathy. Circ J 71:936–940
57. Selby DE, Palmer BM, LeWinter MM et al (2011) Tachycardia-induced diastolic dysfunction and resting tone in myocardium from patients with a normal ejection fraction. J Am Coll Cardiol 58:147–154
58. Paelinck B, Vermeersch P, Stockman D et al (1999) Usefulness of low-dose dobutamine stress echocardiography in predicting recovery of poor left ventricular function in atrial fibrillation dilated cardiomyopathy. Am J Cardiol 83:1668–1671, A1667
59. Ferguson JD, Helms A, Mangrum JM et al (2009) Catheter ablation of atrial fibrillation without fluoroscopy using intracardiac echocardiography and electroanatomic mapping. Circ Arrhythm Electrophysiol 2:611–619
60. Tibayan FA, Lai DT, Timek TA et al (2002) Alterations in left ventricular torsion in tachycardia-induced dilated cardiomyopathy. J Thorac Cardiovasc Surg 124:43–49

61. To AC, Flamm SD, Marwick TH et al (2011) Clinical utility of multimodality LA imaging: assessment of size, function, and structure. JACC Cardiovasc Imaging 4:788–798
62. Schneider C, Malisius R, Krause K et al (2008) Strain rate imaging for functional quantification of the left atrium: atrial deformation predicts the maintenance of sinus rhythm after catheter ablation of atrial fibrillation. Eur Heart J 29:1397–1409
63. Faletra FF, Ho SY, Regoli F et al (2013) Real-time three dimensional transoesophageal echocardiography in imaging key anatomical structures of the left atrium: potential role during atrial fibrillation ablation. Heart 99:133–142
64. Hasdemir C, Yuksel A, Camli D et al (2012) Late gadolinium enhancement CMR in patients with tachycardia-induced cardiomyopathy caused by idiopathic ventricular arrhythmias. Pacing Clin Electrophysiol 35:465–470
65. Matsumoto K, Takahashi N, Ishikawa T et al (2006) Evaluation of myocardial glucose metabolism before and after recovery of myocardial function in patients with tachycardia-induced cardiomyopathy. Pacing Clin Electrophysiol 29:175–180
66. Khasnis A, Jongnarangsin K, Abela G et al (2005) Tachycardia-induced cardiomyopathy: a review of literature. Pacing Clin Electrophysiol 28:710–721
67. Watanabe H, Okamura K, Chinushi M et al (2008) Clinical characteristics, treatment, and outcome of tachycardia induced cardiomyopathy. Int Heart J 49:39–47
68. Aretz HT, Billingham ME, Edwards WD et al (1987) Myocarditis. A histopathologic definition and classification. Am J Cardiovasc Pathol 1:3–14
69. Kindermann I, Barth C, Mahfoud F et al (2012) Update on myocarditis. J Am Coll Cardiol 59:779–792
70. Anzini M, Merlo M, Sabbadini G et al (2013) Long-term evolution and prognostic stratification of biopsy-proven active myocarditis. Circulation 128:2384–2394
71. Imazio M, Trinchero R (2008) Myopericarditis: etiology, management, and prognosis. Int J Cardiol 127:17–26
72. Buiatti A, Merlo M, Pinamonti B et al (2013) Clinical presentation and long-term follow-up of perimyocarditis. J Cardiovasc Med (Hagerstown) 14:235–241
73. Pinamonti B, Alberti E, Cigalotto A et al (1988) Echocardiographic findings in myocarditis. Am J Cardiol 62:285–291
74. Felker GM, Boehmer JP, Hruban RH et al (2000) Echocardiographic findings in fulminant and acute myocarditis. J Am Coll Cardiol 36:227–232
75. Lieback E, Hardouin I, Meyer R et al (1996) Clinical value of echocardiographic tissue characterization in the diagnosis of myocarditis. Eur Heart J 17:135–142
76. Hiramitsu S, Morimoto S, Kato S et al (2001) Transient ventricular wall thickening in acute myocarditis: a serial echocardiographic and histopathologic study. Jpn Circ J 65:863–866
77. Ong P, Athansiadis A, Hill S et al (2011) Usefulness of pericardial effusion as new diagnostic criterion for noninvasive detection of myocarditis. Am J Cardiol 108:445–452
78. Imazio M, Brucato A, Barbieri A et al (2013) Good prognosis for pericarditis with and without myocardial involvement: results from a multicenter, prospective cohort study. Circulation 128:42–49
79. Di Bella G, Coglitore S, Zimbalatti C et al (2008) Strain Doppler echocardiography can identify longitudinal myocardial dysfunction derived from edema in acute myocarditis. Int J Cardiol 126:279–280
80. Hsiao JF, Koshino Y, Bonnichsen CR et al (2013) Speckle tracking echocardiography in acute myocarditis. Int J Cardiovasc Imaging 29:275–284
81. Di Bella G, Gaeta M, Pingitore A et al (2010) Myocardial deformation in acute myocarditis with normal left ventricular wall motion – a cardiac magnetic resonance and 2-dimensional strain echocardiographic study. Circ J 74:1205–1213
82. Escher F, Kasner M, Kuhl U et al (2013) New echocardiographic findings correlate with intramyocardial inflammation in endomyocardial biopsies of patients with acute myocarditis and inflammatory cardiomyopathy. Mediators Inflamm 2013:875420

83. Afonso L, Hari P, Pidlaoan V et al (2010) Acute myocarditis: can novel echocardiographic techniques assist with diagnosis? Eur J Echocardiogr 11:E5
84. Skouri HN, Dec GW, Friedrich MG, Cooper LT (2006) Noninvasive imaging in myocarditis. J Am Coll Cardiol 48:2085–2093
85. Mahrholdt H, Goedecke C, Wagner A et al (2004) Cardiovascular magnetic resonance assessment of human myocarditis: a comparison to histology and molecular pathology. Circulation 109:1250–1258
86. Friedrich MG, Strohm O, Schulz-Menger J et al (1998) Contrast media-enhanced magnetic resonance imaging visualizes myocardial changes in the course of viral myocarditis. Circulation 97:1802–1809
87. Abdel-Aty H, Simonetti O, Friedrich MG (2007) T2-weighted cardiovascular magnetic resonance imaging. J Magn Reson Imaging 26:452–459
88. Friedrich MG, Sechtem U, Schulz-Menger J et al (2009) Cardiovascular magnetic resonance in myocarditis: a JACC White Paper. J Am Coll Cardiol 53:1475–1487
89. De Cobelli F, Pieroni M, Esposito A et al (2006) Delayed gadolinium-enhanced cardiac magnetic resonance in patients with chronic myocarditis presenting with heart failure or recurrent arrhythmias. J Am Coll Cardiol 47:1649–1654
90. Gutberlet M, Spors B, Thoma T et al (2008) Suspected chronic myocarditis at cardiac MR: diagnostic accuracy and association with immunohistologically detected inflammation and viral persistence. Radiology 246:401–409
91. Lurz P, Eitel I, Adam J et al (2012) Diagnostic performance of CMR imaging compared with EMB in patients with suspected myocarditis. JACC Cardiovasc Imaging 5:513–524
92. Iles L, Pfluger H, Phrommintikul A et al (2008) Evaluation of diffuse myocardial fibrosis in heart failure with cardiac magnetic resonance contrast-enhanced T1 mapping. J Am Coll Cardiol 52:1574–1580
93. Dambrin G, Laissy JP, Serfaty JM et al (2007) Diagnostic value of ECG-gated multidetector computed tomography in the early phase of suspected acute myocarditis. A preliminary comparative study with cardiac MRI. Eur Radiol 17:331–338
94. Grun S, Schumm J, Greulich S et al (2012) Long-term follow-up of biopsy-proven viral myocarditis: predictors of mortality and incomplete recovery. J Am Coll Cardiol 59:1604–1615
95. Mahrholdt H, Wagner A, Deluigi CC et al (2006) Presentation, patterns of myocardial damage, and clinical course of viral myocarditis. Circulation 114:1581–1590
96. Maya JD, Orellana M, Ferreira J et al (2010) Chagas disease: present status of pathogenic mechanisms and chemotherapy. Biol Res 43:323–331
97. Nunes MCP, Dones W, Morillo CA, Encina JJ, Ribeiro AL (2013) Chagas disease. An overview of clinical and epidemiological aspects. J Am Coll Cardiol 62:767–776
98. Andrade JP, Marin Neto JA, Paola AA et al (2011) Latin American Guidelines for the diagnosis and treatment of Chagas' heart disease: executive summary. Arq Bras Cardiol 96:434–442
99. Acquatella H (2007) Echocardiography in Chagas heart disease. Circulation 115:1124–1131
100. Viotti RJ, Vigliano C, Laucella S et al (2004) Value of echocardiography for diagnosis and prognosis of chronic Chagas disease cardiomyopathy without heart failure. Heart 90:655–660
101. Garcia-Alvarez A, Sitges M, Regueiro A et al (2011) Myocardial deformation analysis in Chagas heart disease with the use of speckle tracking echocardiography. J Card Fail 17:1028–1034
102. Rochitte CE, Oliveira PF, Andrade JM et al (2005) Myocardial delayed enhancement by magnetic resonance imaging in patients with Chagas' disease: a marker of disease severity. J Am Coll Cardiol 46:1553–1558
103. Regueiro A, Garcia-Alvarez A, Sitges M et al (2011) Myocardial involvement in Chagas disease: insights from cardiac magnetic resonance. Int J Cardiol 165:107–112

104. Nunes MC, Barbosa MM, Ribeiro AL et al (2009) Left atrial volume provides independent prognostic value in patients with Chagas cardiomyopathy. J Am Soc Echocardiogr 22:82–88
105. Nunes MP, Colosimo EA, Reis RC et al (2012) Different prognostic impact of the tissue Doppler-derived E/e' ratio on mortality in Chagas cardiomyopathy patients with heart failure. J Heart Lung Transplant 31:634–641
106. Albini A, Pennesi G, Donatelli F et al (2010) Cardiotoxicity of anticancer drugs: the need for cardio-oncology and cardio-oncological prevention. J Natl Cancer Inst 102:14–25
107. Ky B, Vejpongsa P, Yeh ET et al (2013) Emerging paradigms in cardiomyopathies associated with cancer therapies. Circ Res 113:754–764
108. Sawaya H, Sebag IA, Plana JC et al (2011) Early detection and prediction of cardiotoxicity in chemotherapy-treated patients. Am J Cardiol 107:1375–1380
109. Yeh ET, Tong AT, Lenihan DJ et al (2004) Cardiovascular complications of cancer therapy: diagnosis, pathogenesis, and management. Circulation 109:3122–3131
110. Lipshultz SE, Adams MJ, Colan SD et al (2013) Long-term cardiovascular toxicity in children, adolescents, and young adults who receive cancer therapy: pathophysiology, course, monitoring, management, prevention, and research directions: a scientific statement from the American Heart Association. Circulation 128:1927–1995
111. Oreto L, Todaro MC, Umland MM et al (2012) Use of echocardiography to evaluate the cardiac effects of therapies used in cancer treatment: what do we know? J Am Soc Echocardiogr 25:1141–1152
112. Drafts BC, Twomley KM, D'Agostino R Jr et al (2013) Low to moderate dose anthracycline-based chemotherapy is associated with early noninvasive imaging evidence of subclinical cardiovascular disease. JACC Cardiovasc Imaging 6:877–885
113. Armstrong GT, Plana JC, Zhang N et al (2012) Screening adult survivors of childhood cancer for cardiomyopathy: comparison of echocardiography and cardiac magnetic resonance imaging. J Clin Oncol 30:2876–2884
114. Ylanen K, Poutanen T, Savikurki-Heikkila P et al (2013) Cardiac magnetic resonance imaging in the evaluation of the late effects of anthracyclines among long-term survivors of childhood cancer. J Am Coll Cardiol 61:1539–1547
115. Neilan TG, Coelho-Filho OR, Pena-Herrera D et al (2012) Left ventricular mass in patients with a cardiomyopathy after treatment with anthracyclines. Am J Cardiol 110:1679–1686
116. Tham EB, Haykowsky MJ, Chow K et al (2013) Diffuse myocardial fibrosis by T1-mapping in children with subclinical anthracycline cardiotoxicity: relationship to exercise capacity, cumulative dose and remodeling. J Cardiovasc Magn Reson 15:48
117. Neilan TG, Coelho-Filho OR, Shah RV et al (2013) Myocardial extracellular volume by cardiac magnetic resonance imaging in patients treated with anthracycline-based chemotherapy. Am J Cardiol 111:717–722
118. Fallah-Rad N, Lytwyn M, Fang T et al (2008) Delayed contrast enhancement cardiac magnetic resonance imaging in trastuzumab induced cardiomyopathy. J Cardiovasc Magn Reson 10:5
119. de Geus-Oei LF, Mavinkurve-Groothuis AM, Bellersen L et al (2011) Scintigraphic techniques for early detection of cancer treatment-induced cardiotoxicity. J Nucl Med 52:560–571
120. Valdes Olmos RA, ten Bokkel Huinink WW, ten Hoeve RF et al (1994) Usefulness of indium-111 antimyosin scintigraphy in confirming myocardial injury in patients with anthracycline-associated left ventricular dysfunction. Ann Oncol 5:617–622
121. Elliott P, Andersson B, Arbustini E et al (2008) Classification of the cardiomyopathies: a position statement from the European Society of Cardiology Working Group on Myocardial and Pericardial Diseases. Eur Heart J 29:270–276
122. Chin TK, Perloff JK, Williams RG et al (1990) Isolated noncompaction of left ventricular myocardium. A study of eight cases. Circulation 82:507–513

123. Oechslin EN, Attenhofer Jost CH, Rojas JR et al (2000) Long-term follow-up of 34 adults with isolated left ventricular noncompaction: a distinct cardiomyopathy with poor prognosis. J Am Coll Cardiol 36:493–500
124. Oechslin E, Jenni R (2011) Left ventricular noncompaction revisited: a distinct phenotype with genetic heterogeneity? Eur Heart J 32:1446–1456
125. Aras D, Tufekcioglu O, Ergun K et al (2006) Clinical features of isolated ventricular noncompaction in adults long-term clinical course, echocardiographic properties, and predictors of left ventricular failure. J Card Fail 12:726–733
126. Pignatelli RH, McMahon CJ, Dreyer WJ et al (2003) Clinical characterization of left ventricular noncompaction in children: a relatively common form of cardiomyopathy. Circulation 108:2672–2678
127. Jenni R, Goebel N, Tartini R et al (1986) Persisting myocardial sinusoids of both ventricles as an isolated anomaly: echocardiographic, angiographic, and pathologic anatomical findings. Cardiovasc Intervent Radiol 9:127–131
128. Thavendiranathan P, Dahiya A, Phelan D et al (2013) Isolated left ventricular noncompaction controversies in diagnostic criteria, adverse outcomes and management. Heart 99:681–689
129. Paterick TE, Tajik AJ (2012) Left ventricular noncompaction: a diagnostically challenging cardiomyopathy. Circ J 76:1556–1562
130. Boyd MT, Seward JB, Tajik AJ et al (1987) Frequency and location of prominent left ventricular trabeculations at autopsy in 474 normal human hearts: implications for evaluation of mural thrombi by two-dimensional echocardiography. J Am Coll Cardiol 9:323–326
131. Jenni R, Oechslin E, Schneider J et al (2001) Echocardiographic and pathoanatomical characteristics of isolated left ventricular noncompaction: a step towards classification as a distinct cardiomyopathy. Heart 86:666–671
132. Stollberger C, Finsterer J, Blazek G (2002) Left ventricular hypertrabeculation/noncompaction and association with additional cardiac abnormalities and neuromuscular disorders. Am J Cardiol 90:899–902
133. Stollberger C, Finsterer J (2004) Left ventricular hypertrabeculation/noncompaction. J Am Soc Echocardiogr 17:91–100
134. Finsterer J, Stollberger C (2011) No rationale for a diagnostic ratio in left ventricular hypertrabeculation/noncompaction. Int J Cardiol 146:91–92
135. Frischknecht BS, Attenhofer Jost CH, Oechslin EN et al (2005) Validation of noncompaction criteria in dilated cardiomyopathy, and valvular and hypertensive heart disease. J Am Soc Echocardiogr 18:865–872
136. Belanger AR, Miller MA, Donthireddi UR et al (2008) New classification scheme of left ventricular noncompaction and correlation with ventricular performance. Am J Cardiol 102:92–96
137. Kohli SK, Pantazis AA, Shah JS et al (2008) Diagnosis of left-ventricular noncompaction in patients with left-ventricular systolic dysfunction: time for a reappraisal of diagnostic criteria? Eur Heart J 29:89–95
138. Saleeb SF, Margossian R, Spencer CT et al (2012) Reproducibility of echocardiographic diagnosis of left ventricular noncompaction. J Am Soc Echocardiogr 25:194–202
139. Gati S, Chandra N, Bennett RL et al (2013) Increased left ventricular trabeculation in highly trained athletes: do we need more stringent criteria for the diagnosis of left ventricular noncompaction in athletes? Heart 99:401–408
140. de Groot-de Laat LE, Krenning BJ, ten Cate FJ et al (2005) Usefulness of contrast echocardiography for diagnosis of left ventricular noncompaction. Am J Cardiol 95:1131–1134
141. Maltagliati A, Pepi M (2000) Isolated noncompaction of the myocardium: multiplane transesophageal echocardiography diagnosis in an adult. J Am Soc Echocardiogr 13:1047–1049
142. Bellavia D, Michelena HI, Martinez M et al (2010) Speckle myocardial imaging modalities for early detection of myocardial impairment in isolated left ventricular noncompaction. Heart 96:440–447

143. van Dalen BM, Caliskan K, Soliman OI et al (2008) Left ventricular solid body rotation in noncompaction cardiomyopathy: a potential new objective and quantitative functional diagnostic criterion? Eur J Heart Fail 10:1088–1093
144. van Dalen BM, Caliskan K, Soliman OI et al (2011) Diagnostic value of rigid body rotation in noncompaction cardiomyopathy. J Am Soc Echocardiogr 24:548–555
145. Peters F, Khandheria BK, Libhaber E et al (2014) Left ventricular twist in left ventricular noncompaction. Eur Heart J Cardiovasc Imaging 15:48–55
146. Niemann M, Liu D, Hu K et al (2012) Echocardiographic quantification of regional deformation helps to distinguish isolated left ventricular noncompaction from dilated cardiomyopathy. Eur J Heart Fail 14:155–161
147. Caselli S, Autore C, Serdoz A et al (2012) Three-dimensional echocardiographic characterization of patients with left ventricular noncompaction. J Am Soc Echocardiogr 25:203–209
148. Bodiwala K, Miller AP, Nanda NC et al (2005) Live three-dimensional transthoracic echocardiographic assessment of ventricular noncompaction. Echocardiography 22:611–620
149. Petersen SE, Selvanayagam JB, Wiesmann F et al (2005) Left ventricular noncompaction: insights from cardiovascular magnetic resonance imaging. J Am Coll Cardiol 46:101–105
150. Kawel N, Nacif M, Arai AE et al (2012) Trabeculated (noncompacted) and compact myocardium in adults: the multi-ethnic study of atherosclerosis. Circ Cardiovasc Imaging 5:357–366
151. Korcyk D, Edwards CC, Armstrong G et al (2004) Contrast-enhanced cardiac magnetic resonance in a patient with familial isolated ventricular noncompaction. J Cardiovasc Magn Reson 6:569–576
152. Jacquier A, Thuny F, Jop B et al (2010) Measurement of trabeculated left ventricular mass using cardiac magnetic resonance imaging in the diagnosis of left ventricular noncompaction. Eur Heart J 31:1098–1104
153. Grothoff M, Pachowsky M, Hoffmann J et al (2012) Value of cardiovascular MR in diagnosing left ventricular noncompaction cardiomyopathy and in discriminating between other cardiomyopathies. Eur Radiol 22:2699–2709
154. Captur G, Flett AS, Jacoby DL et al (2013) Left ventricular nonnoncompaction: the mitral valve prolapse of the 21st century? Int J Cardiol 164:3–6
155. Nucifora G, Aquaro GD, Pingitore A et al (2011) Myocardial fibrosis in isolated left ventricular noncompaction and its relation to disease severity. Eur J Heart Fail 13:170–176
156. Dodd JD, Holmvang G, Hoffmann U et al (2007) Quantification of left ventricular noncompaction and trabecular delayed hyperenhancement with cardiac MRI: correlation with clinical severity. AJR Am J Roentgenol 189:974–980
157. Dursun M, Agayev A, Nisli K et al (2010) MR imaging features of ventricular noncompaction: emphasis on distribution and pattern of fibrosis. Eur J Radiol 74:147–151
158. Junqueira FP, Fernandes FD, Coutinho AC et al (2009) Case report. Isolated left ventricular myocardiumnoncompaction: MR imaging findings from three cases. Br J Radiol 82:e37–e41
159. Melendez-Ramirez G, Castillo-Castellon F, Espinola-Zavaleta N et al (2012) Left ventricular noncompaction: a proposal of new diagnostic criteria by multidetector computed tomography. J Cardiovasc Comput Tomogr 6:346–354
160. Sidhu MS, Uthamalingam S, Ahmed W et al (2014) Defining left ventricular noncompaction using cardiac computed tomography. J Thorac Imaging 29:60–66
161. Jenni R, Wyss CA, Oechslin EN et al (2002) Isolated ventricular noncompaction is associated with coronary microcirculatory dysfunction. J Am Coll Cardiol 39:450–454
162. Stanton C, Bruce C, Connolly H et al (2009) Isolated left ventricular noncompaction syndrome. Am J Cardiol 104:1135–1138
163. McMahon CJ, Pignatelli RH, Nagueh SF et al (2007) Left ventricular noncompaction cardiomyopathy in children: characterisation of clinical status using tissue Doppler-derived indices of left ventricular diastolic relaxation. Heart 93:676–681
164. Wald R, Veldtman G, Golding F et al (2004) Determinants of outcome in isolated ventricular noncompaction in childhood. Am J Cardiol 94:1581–1584

165. Punn R, Silverman NH (2010) Cardiac segmental analysis in left ventricular noncompaction: experience in a pediatric population. J Am Soc Echocardiogr 23:46–53
166. McMurray JJ, Adamopoulos S, Anker SD et al (2012) ESC Guidelines for the diagnosis and treatment of acute and chronic heart failure 2012: The Task Force for the Diagnosis and Treatment of Acute and Chronic Heart Failure 2012 of the European Society of Cardiology. Developed in collaboration with the Heart Failure Association (HFA) of the ESC. Eur Heart J 33:1787–1847